FFI-RAPPORT

18/00886

SAR ship detection in dual polarization combination channels

Øyvind Kinden Lensjø

SAR ship detection in dual polarization combination channels

Øyvind Kinden Lensjø

Norwegian Defence Research Establishment (FFI) 16 May 2018

Keywords

Maritim overvåking
Satellitter
Syntetisk apertur–radar (SAR)
Skipsdeteksjon

FFI-rapport
FFI-RAPPORT 18/00886

Prosjektnummer
144102

ISBN
P: 978-82-464-3064-5
E: 978-82-464-3065-2

Approved by
Richard Olsen, *Research Manager*
Johnny Bardal, *Director*

Summary

Satellite Synthetic Aperture Radar (SAR) imagery is widely used for automatic ship detection. SAR data comes in different modes and polarization combinations. Dual polarization ScanSAR products offer good spatial coverage, and are thus often the mode of choice. Dual polarization SAR products consist of a co-pol and a cross-pol image. Utilizing the full potential of the data is an important aspect in any surveillance task. In this study, two dual polarization channel combinations are presented and evaluated for use in automatic ship detection. The first one, named *dual*, is a multiplication of the individual polarization amplitudes, scaled with an estimated average sea background. The second combination channel, named *dual-int*, is a multiplication of the individual polarization channel intensities. Both channels aim to increase the ship-to-sea contrast in the SAR data, as one of the main objectives is to detect bright pixels in the images. Data from two platforms, RADARSAT-2 and Sentinel-1, have been investigated in this study.

A short state-of-the-art literature review on dual polarization channel combinations in automatic ship detection has been done to put the presented methods in context.

The statistical properties of the different channels used in the automatic ship detection have been investigated. The RADARSAT-2 data fits well with the proposed probability density functions (PDFs), while the Sentinel-1 data fits the PDFs to a lesser degree. Recommendation on a more in-depth analysis of the statistics of Sentinel-1 SAR data is made.

Results from the automatic ship detection show that both dual polarization combination channels generally outperform the co-pol channel in terms of identified ship detection counts. Comparison with the cross-pol channel shows similar performance for both presented dual polarization combination channels. When looking at the added value provided by the proposed channels, results differ between the two platforms. For RADARSAT-2, both the dual and the dual-int channel offer added value in terms of an increase in the number of identified detections. This is not the case for Sentinel-1. However, the detections can still be used in an updated confidence estimate procedure for both platforms.

Analysis of the false alarm rate results shows that the combination channels both perform worse than the cross-pol channel. Two special cases in which the co-pol channel is known to produce many false alarms have been investigated. At low wind conditions, patterns in the SAR co-pol image due to algae growth can produce high false alarm rates. It is shown that this problem does not seem to persist in the combination channels. Secondly, false alarms at low incidence angles are common in the co-pol channel. Both combination channels have fewer false alarms than the co-pol channel, but the counts are still very high.

Comparing the two presented combination channels, the *dual* channel comes out best and recommendations are made to use this channel. Also, if timing is crucial, it is recommended only to process the cross-pol and the dual channel for RADARSAT-2 imagery, and only the co-pol and cross-pol channels for Sentinel-1 imagery.

Sammendrag

Bruk av bilder fra satellittbåren syntetisk apertur-radar (SAR) er utbredt i automatisk skipsdeteksjon. SAR-data leveres i en rekke forskjellige modi og polarisasjonskombinasjoner. Dual-polarisasjon ScanSAR-produkter dekker store områder og er følgelig ofte den foretrukne modusen. Disse produktene inneholder ett ko-pol- og ett kryss-pol-bilde. Ved bruk i maritim overvåking er det viktig å kunne utnytte dataens fulle potensial. Denne studien presenterer og evaluerer to sammensatte dual-polarisasjonskanaler for bruk i automatisk skipsdeteksjon. Den første, kalt *dual*, er produktet av de individuelle polarisasjonskanalenes amplitudeverdier, skalert med en estimert gjennomsnittlig sjøbakgrunn. I den andre kanalen, kalt *dual-int*, multipliseres de individuelle polarisasjonskanalenes intensitetsverdier. Målet med disse sammensatte kanalene er å øke kontrasten mellom skip og sjø i SAR-bildene, da et av de viktigste aspektene i automatisk skipsdeteksjon er deteksjon av lyse piksler i bildene. Data fra to plattformer, RADARSAT-2 og Sentinel-1, har blitt brukt i studien.

En kort state-of-the-art litteraturstudie på sammensatte dual-polarisasjonskanaler i automatisk skipsdeteksjon har blitt gjennomført for å sette de presenterte metodene i kontekst.

Statistiske egenskaper hos de ulike kanalene brukt i skipsdeteksjonen har blitt undersøkt. Sannsynlighetstetthetsfunksjonene (PDFene) brukt i skipsdeteksjonen viste seg å passe godt for data fra RADARSAT-2. Data fra Sentinel-1 passet imidlertid i mindre grad. Det anbefales følgelig å gjøre en mer grundig studie på de statistiske egenskapene til SAR-data fra Sentinel-1.

Resultatene fra den automatiske skipsdeteksjonen viser at begge sammensatte kanaler yter bedre enn ko-pol-kanalen. Sammenlignet med kryss-pol-kanalen ligger ytelsen generelt sett på samme nivå. Ser man så på den oppnådde merinformasjonen ved bruk av de sammensatte kanalene, spriker resultatene med hensyn på plattform. For RADARSAT-2 tilbyr begge de sammensatte kanalene merinformasjon i form av økt antall identifiserte skip. Dette er ikke tilfellet for Sentinel-1. Det gjøres imidlertid oppmerksom på at skipsdeteksjoner fra de sammensatte kanalene også kan brukes i et oppdatert konfidensmål for deteksjoner hos begge plattformer.

Analysen av falske alarmer viser at begge de sammensatte kanalene yter dårligere enn kryss-pol-kanalen. To spesialtilfeller tar for seg kjente problemstillinger med tanke på falske alarmer i ko-pol-kanalen. Lave vindforhold kan føre til algevekst på havoverflaten. Dette manifesterer seg som velkjente mønstre i radarbildene og kan føre til mange falske alarmer. Dette problemet overføres ikke til de sammensatte kanalene, viser tilfellene analysert i denne studien. Videre ser man ofte flere falske alarmer i ko-pol ved lave innfallsvinkler. De sammensatte kanalene gir færre falske alarmer ved lave innfallsvinkler sammenlignet med ko-pol, men de rapporterte tallene er fortsatt høye.

En sammenligning av det to presenterte sammensatte kanalene viser at *dual* har best ytelse. Det anbefales følgelig å bruke denne kanalen. Ved tidskritiske operasjoner anbefales det å kun prosessere kryss-pol og dual for RADARSAT-2, samt ko-pol og kryss-pol for Sentinel-1.

Content

Preface

The work presented in this report is carried out in FFI project 144102. The report is a deliverable in work package 1, “Dual-pol ship detection”, under Norwegian Space Center contract “Ship detection and surveillance from satellite”, JOP.03.17.4. FFI and Kongsberg Satellite Services (KSAT) have been responsible for this work package.

1 Introduction

Utilizing the full potential of the input data is an important aspect of any surveillance task. When using Synthetic Aperture Radar (SAR) data for ship detection, different polarizations will display the same scene, but the information contained in the individual polarization channels will differ. Hence, it is of interest to investigate the possibilities arising from the individual channels as well as their combinations. Fully polarimetric SAR data presents the most extensive foundation on which to retrieve data from both individual channels and combinations thereof. However, the spatial coverage of fully polarimetric SAR data is limited. Hence, dual polarization products, offering higher spatial coverage, are more often used in operational SAR ship detection. This study presents two different ways of combining the individual polarization channels for dual polarization SAR data, and compares them with the individual channels' performance. Only multi-look intensity (ground range detected) products are considered. The outline of the study is as follows:

- Chapter 1 presents a brief background on ship detection in SAR imagery, along with descriptions of the SAR satellites used in the study. Also, the dual polarization channel combinations are presented.

- Chapter 2 presents a short state-of-the-art literature review on SAR dual polarization channel combinations.

- Chapter 3 details the methodology employed in the study. This includes a description of the automatic ship detection tool, a closer look at the statistical properties of the different channels and channel combinations, a presentation of the data test set used and finally a description of the ground truth tool employed.

- Chapter 4 presents the obtained results and a corresponding analysis.

- Chapter 5 ends the study with a discussion of the results as well as recommendations on how to best use the knowledge acquired in the study.

1.1 Background

The SAR satellite ERS-1 was launched by the European Space Agency (ESA) in 1991. Since then, SAR imagery has been used extensively for maritime monitoring of the vast Norwegian ocean areas [1, 2], both in terms of ship and oil spill detection. Having the advantages of large area coverage and operational independence of weather and daylight, satellite SAR imagery can monitor these ocean areas efficiently. The Norwegian Armed Forces and the Norwegian Coastal Administration (NCA) have both used SAR data from the Canadian RADARSAT-1 and -2 operationally for many years, and with the launch of ESA's Sentinel-1A and -1B (2014 and 2016), the availability of SAR imagery for maritime monitoring is historically high. This includes data from other SAR platform such as e.g. TerraSar-X and COSMO- SkyMed, but the

focus in this study will be on RADARSAT-2 and Sentinel-1, due to the fact that these two platforms are the primary sources of SAR data in the monitoring of Norwegian ocean areas.

SAR sensors have different modes of operation, each with different characteristics in terms of e.g. resolution, swath widths, polarization combinations and pixel spacing. The different polarization combinations stems from the SAR instrument's ability to transmit and receive linearly polarized signals in the following combinations:

- HH: Horizontally polarized transmit and receive
- VV: Vertically polarized transmit and receive
- HV: Horizontally polarized transmit and vertically polarized receive
- VH: Vertically polarized transmit and horizontally polarized receive

The former two combinations are known as co-pol, the latter two as cross-pol. Data acquisition can be done in single polarization (HH, VV, HV or VH), dual polarization (HH and HV, VV and VH or HH and VV) or quad-polarization (HH, VV, HV and VH). Some SAR satellites (e.g. the Indian RISAT and the upcoming RADARSAT Constellation Mission) use circular polarized signals. However, such products are not applicable for this study and are thus left out in the following.

For maritime surveillance, different ScanSAR modes are mostly used. ScanSAR images cover large areas with the obvious trade-off of having course resolution. The most common polarization combination for ScanSAR products are the dual polarization combinations HH+HV and VV+VH. The following two sections present the key information on RADARSAT-2 and Sentinel-1 products used in this study.

1.2 RADARSAT-2

The Canadian SAR satellite RADARSAT-2 was launched December 14th 2007. Operating in a near sun-synchronous polar orbit with an inclination angle of 98.6°, RADARSAT-2 covers the Norwegian ocean areas well. The satellite altitude is 798 km above Earth, giving an orbital period of 100.7 minutes. The SAR instrument operates in C-band (5.405 GHz). Data acquisition can be done in single polarization (HH, VV, HV or VH), dual polarization (HH and HV or VV and VH) or quad-polarization (HH, HV, VH and VV). The SAR instrument can be set to operate in a number of different modes, depending on the desired product. As explained above, ScanSAR data is the mode of choice in this study. Table 1.1 below shows the key information for the two RADARSAT-2 modes used in this study. For in depth evaluation of RADARSAT-2 in ship detection, see [3].

Table 1.1 RADARSAT-2 ScanSAR key information.

Mode	Approximate nominal swath width	Approximate resolution in range	Approximate resolution in azimuth	Approximate incidence angle	Polarization
ScanSAR Narrow	300 km	37.7-79.9 m	60 m	20-47°	Single-pol or dual-pol
ScanSAR Wide	450-500 km	72.1-160 m	100 m	20-49°	

1.3 Sentinel-1A and -1B

ESA's SAR satellites Sentinel-1A and -1B were launched April 3rd 2014 and April 25th 2016, respectively. Both satellites are in sun-synchronous polar orbits at 98.18° inclination angle, 180° apart in the orbital plane. The satellites have an altitude of 693 km above Earth, giving an orbital time of 98.6 minutes. As for RADARSAT-2, the Sentinel SAR instrument operates at C-band frequency 5.405 GHz, and can transmit and receive linearly polarized signals. Data acquisition can be done in single polarization (HH or VV) or dual polarization (HH and HV or VV and VH). The Sentinel-1 satellites have 4 modes of operation, two of which are used in this study, the Interferometric Wide (IW) swath and the Extra Wide (EW) swath. These two modes use a technique called Terrain Observation with Progressive Scans SAR (TOPSAR), which is a form of ScanSAR imaging. For more info on TOPSAR processing see [4]. Table 1.2 below shows key information on Sentinel-1 modes IW and EW. Note that single polarization now means HH or VV (single polarization cross-pol HV or VH is not available). For more info on the Sentinel-1A and -1B missions see [5, 6].

Table 1.2 Sentinel-1A and -1B IW and EW key information.

Mode	Approximate nominal swath width	Approximate resolution in range	Approximate resolution in azimuth	Approximate incidence angle	Polarization
IW	250 km	20 m (High) 88 m (Medium)	22 m (High) 87 m (Medium)	29.1-46°	Single-pol or dual-pol
EW	400 km	50 m (High) 93 m (Medium)	50 m (High) 87 m (Medium)	18.9-47°	

1.4 Dual pol channel combinations

In [7], Hannevik, Eldhuset and Olsen outline the importance of polarization when doing ship detection in SAR imagery. As the scattering properties in different polarization channels vary with the materials and surfaces being imaged, the resulting SAR images will differ. As an example, it is shown how the ship-to-sea contrast in co-pol is generally greater at high incidence angles due to low backscatter from the ocean, while the contrast measure for cross-pol is less dependent on both imaging geometry and wind. Also, the complexity of a ship's superstructure plays an important role in the backscatter mechanisms. In addition to looking at the ship-to-sea contrast for co-pol and cross-pol, a combined channel from dual pol SAR imagery is investigated. This channel is based in the work presented by Olsen, Eldhuset, Helleren and Brekke in [8]. The objective in [8] was to increase the contrast between bright targets (e.g. land or ships) and the background (sea). The resulting dual-pol channel was written as:

$$\frac{co-pol * cross-pol}{C} \tag{1.1}$$

The co-pol and cross-pol terms are amplitude values, thus the result is in the intensity domain. The constant C was in [8] used to rescale the cross-pol channel to provide a similar mean value to the co-pol channel. In this study and in [7], C represents an estimated averaged sea background from the two polarization channels. Hannevik *et al.* show clearly how the ship-to-sea contrast for the dual pol combination channel in most cases is higher when compared with the individual channels. This result is of course very interesting when doing ship detection, as one of the prime objectives is to detect bright pixels in the images. An example of the increase in contrast is shown in Figure 1.1. This is taken from a RADARSAT-2 ScanSAR Wide product acquired August 18th 2017. Displayed in the figure are the amplitude signatures of a vessel at incidence angle 36.6°. The top plot is HH, the middle HV and the bottom is the dual pol combination channel described above. The z-axis on the top two has maximum 20000, while the bottom one has maximum 60000. It is clear that the contrast in the combined channel is greater than for the individual channels. The combined channel is referred to as dual in the following.

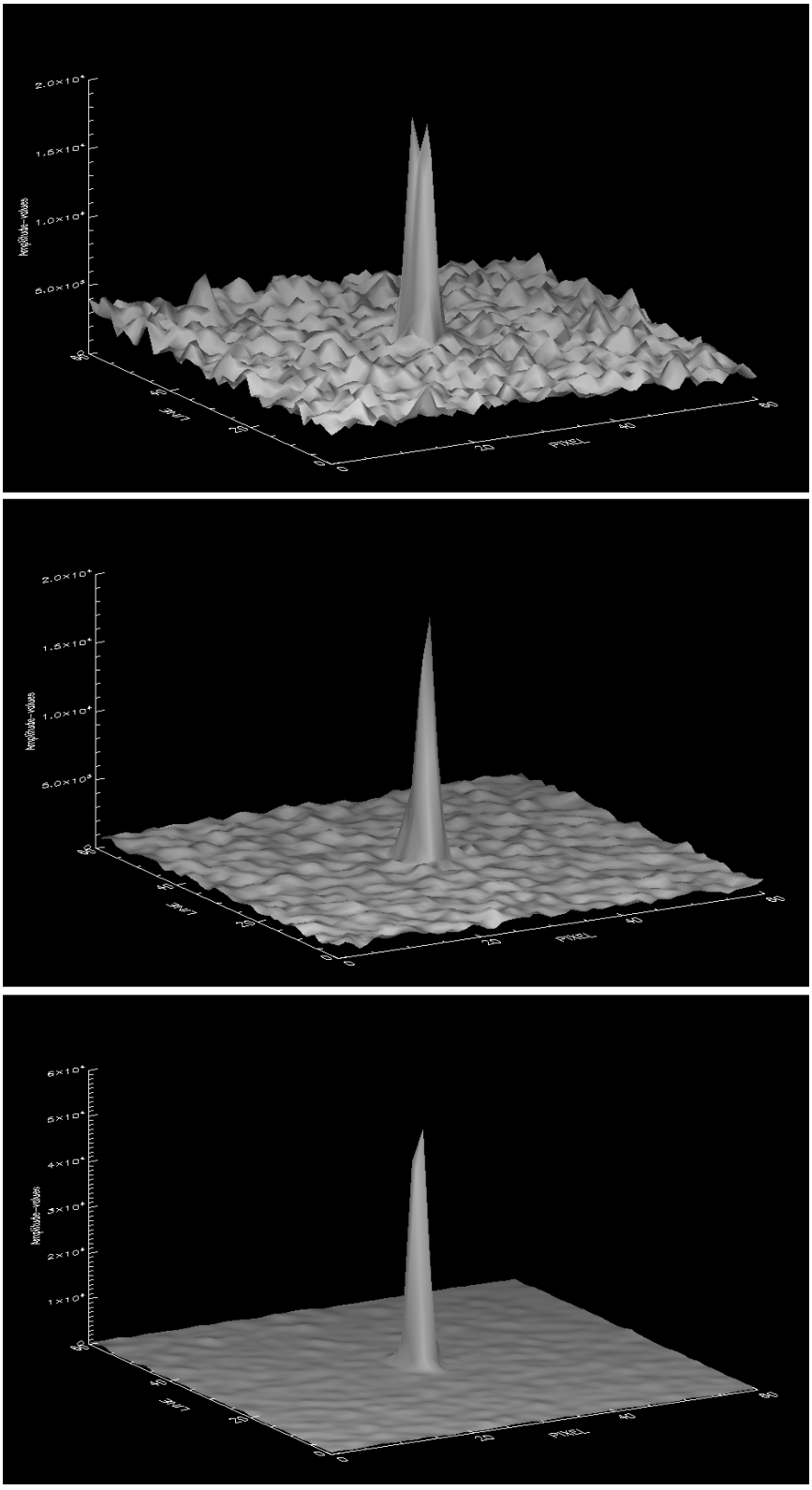

Figure 1.1 Ship-to-sea contrast. Top: HH Middle: HV Bottom: dual.

In addition to the dual channel described above, another combination of the single polarization channels has been investigated in this study. With the contrast enhancement in mind, the square of the dual channel represents a new channel with a potential for even greater ship-to-sea contrasts. The dual-int channel is hence calculated in the following manner:

$$\frac{co-pol*co-pol*cross-pol*cross-pol}{C^2} \tag{1.2}$$

Again, the co-pol and cross-pol terms are in amplitude values, yielding the result in squared intensity. The constant C is now set to 1.

The ship detection performance of these two combined dual polarization channels is investigated in this study. This includes an analysis of false alarms and the impact detections from the combined channels can have on confidence measurements.

2 Literature review

This literature review aims at giving a short introduction to the state-of-the-art in dual polarization channel combination used in ship detection. The focus is on ground range products as the main topic of the study is to investigate the performance of two dual polarization combination channels for such SAR products. Note that the literature review is considered informative only – no results obtained in the study will be compared with the methods described in this chapter.

In [9], Liu presents a ship detection method that is a combination of the Likelihood Ratio Test (LRT) with K-distribution constant false alarm rate (KCFAR) detection. The method is designed for multi-look processed intensity data and is a continuation of the work presented on SAR single look complex (SLC) data in [10]. The decision variable presented in the study is given by:

$$\frac{R_1}{C_{11o}}+\frac{R_2}{C_{22o}}=\begin{cases}>\eta' \text{ for a ship}\\ \leq\eta' \text{ for ocean}\end{cases} \tag{2.1}$$

where R_1 and R_2 are the multi-look intensity variables of the scattering vector components S_{HH} and S_{HV}, given by:

$$R_1=\frac{1}{n}\sum_{k=1}^{n}\left|S_{HH}(k)\right|^2, \qquad \mathrm{R}_2=\frac{1}{n}\sum_{k=1}^{n}\left|S_{HV}(k)\right|^2 \tag{2.2}$$

C_{11o} and C_{22o} are ocean covariance and η' is a threshold determined by the probability of false alarm (P_{FA}). The decision variable is referred to as the normalized intensity sum (NIS). The detection threshold is found by modeling the ocean samples as a K-distribution probability density function and setting a certain P_{FA}.

The method has been tested on two RADARSAT-2 Ocean Surveillance, Very wide swath, Near incidence angle (OSVN) mode products. Both products are dual polarization HH/HV. Ground truth is provided by Automatic Identification System (AIS) data. Detection results show an improvement in the probability of detection compared to single-channel ship detection (HH only, HV only and the union of HH and HV). However, there is no evident improvement in the rate of false alarms (HV has fewer false alarms in both tests).

As stated above, in [10], Liu *et al.* presents a ship detection method for SLC products. However, results from dual-polarized amplitude products are included for comparison. The dual-polarized amplitude products used are simply the magnitude of the SLC products. Single-polarization ship detection is also done. Thus, even though the method is designed for SLC data, a comparison of single- and dual-polarized amplitude products is made. The decision variables presented are found by using the LRT approach. SAR data used in the study was acquired by the Canadian EC CV-580 SAR system, a flight mounted system. Results show that the dual-polarized amplitude only combinations HH/HV and VV/VH perform better than single-polarized co-pol (HH, VV). For single-polarized cross-pol (HV, VH), the reported performance is better than or equal to dual-polarized amplitude only for low incidence angles. For large incidence angles, the dual-polarized data also outperforms single-polarized cross-pol channels. In [11], Crisp uses the decision variable suggested in [10] for the dual-polarized amplitude only data on RADARSAT-2 ScanSAR Narrow dual-polarized multi-look products and reports very poor results. Crisp suggests that as the method in [10] is designed for SLC data with the assumption that the data has a zero mean circularly symmetric complex Gaussian distribution, it is not well suited for multi-look SAR data.

In [11], Crisp uses RADARSAT-2 ScanSAR Narrow HH/HV multi-look imagery to investigate the best way to combine the HH and HV channels in ship detection. Each method presented consists of defining one or more decision variable and applying a moving window CFAR detector to each of them. The CFAR detector is the same for all methods and assumes that the ocean has Gaussian statistics in the dB domain. In cases where more than one decision variable were used, the results from the individual decision variables were pooled subsequent to individual ship detection. The following channel combination methods were presented:

1. **HH-or-HV**: Detections done in HH and HV pooled
2. **HH-and-HV**: Detections done in both single-polarized channels
3. **HH-times-HV**: $\sqrt{|HH| * |HV|}$, where $|HH|$ and $|HV|$ are intensities
4. **HH-times-HV or HV**: Detections done in fused channel and HV pooled

5. **GM-or-HH-or-HV**: The GM decision variable was designed to take advantage of the common assumption that the HH and HV backscatter are more highly correlated for ships than for the surrounding sea. The individual channels are first converted to the dB domain yielding X_1 and X_2, then normalized and summed to produce $(X_1 - \mu_1)/\sigma_1 + (X_2 - \mu_2)/\sigma_2$. μ_i and σ_i are the mean and standard deviation of X_i. X_1 and X_2 are further assumed to be jointly Gaussian leading to the decision variable:

$$\frac{1}{\sqrt{2(1+\rho)}}\left(\frac{X_1-\mu_1}{\sigma_1}+\frac{X_2-\mu_2}{\sigma_2}\right) \tag{2.3}$$

   where ρ is the correlation coefficient. μ_i, σ_i and ρ are estimated from the background ocean using a moving CFAR window. The detections from this decision variable are then pooled with the HH and HV detections.

6. **HH-only**: Single-polarized co-pol channel for comparison

7. **HV-only**: Single-polarized cross-pol channel for comparison

Results show that using both channels in the detection process improves performance significantly. Channel combinations 1, 3 and 4 perform substantially better than the single-pol methods for all desired P_{FA}. Option 5 also performs better than the single-pol channels, but not as well as the aforementioned combinations. This is due to threshold being set to ensure the GM decision variable plays an active role in the combination of decision variables. The best single decision variable is number 3, while the best overall performers are number 1 and 4. Note that optimization of the CFAR window and clustering parameters was done in the study, and the author states that the results should be considered indicative only.

Smith *et al* takes advantage of the correlation between the polarization channels when analyzing Envisat Advanced Synthetic Aperture Radar (ASAR) HH/HV data in [12]. A CFAR ship detector based on mean amplitude and amplitude rms is presented. The correlation coefficient ρ between the two channels is then used to adjust the CFAR threshold. They observed that ρ is higher for pixels containing ships compared with clutter pixels. The HH decision variable is thus divided by $1 - \rho$ allowing a higher CFAR threshold with no degradation in detection performance. The reported false alarm rate is reduced when employing this technique.

In [13], Li *et al.* investigates fusion methods of Envisat ASAR alternating polarization mode data for improved performance in ship detection. Both SLC and detected (multi-looked amplitude) products are treated individually. Analysis of SLC and detected combination HH/VV is not applicable for this study and is thus not presented here. The fusion method presented is a multiplication of the co-pol and cross-pol channels (HH*HV and VV*VH). The ship detection method employed is a hollow stencil order statistic CFAR. Ground truth is not available and performance measurements are thus based purely on visual interpretation. The presented figure shows that the fused channel has a much more depressed background than the two single-pol channels.

Pelich *et al.* present a dual-polarization method with fused channels which avoids employing the often computationally demanding sliding window CFAR approach [14]. The geometric and quadratic mean of the SAR amplitude values, given by:

$$\begin{cases} M_0 = \sqrt{xy} \\ M_2 = \sqrt{\dfrac{x^2 + y^2}{2}} \end{cases} \tag{2.4}$$

where x and y represent the amplitude values of the co-pol and cross-pol SAR product (e.g. VV and VH). The channels are considered independent and the joint probability density function (PDF) of M_0 and M_2 is found ($p(M_0, M_2)$). SAR single look images are analyzed in the study and the amplitude values are thus expected to follow Rayleigh distributions. Only clutter samples are used to estimate the parameters of the joint PDF, hence a coarse detection of ship samples is needed ahead of this. The decision variable presented is given by:

$$p(M_0, M_2) = \begin{cases} < \tau \text{ for a ship} \\ \geq \tau \text{ for the ocean} \end{cases} \tag{2.5}$$

The threshold value τ is found by choosing a P_{FA} and solving

$$P_{FA} = \iint\limits_{p(M_0, M_2) < \tau} p(M_0, M_2) \mathrm{d}M_0 \mathrm{d}M_2 \tag{2.6}$$

Sentinel-1 IW VV/VH single-look amplitude products are used to evaluate the ship detector proposed. Results from three image patches with P_{FA} set to 10^{-8} are presented. The patches contain ships varying in size from less than 20 m to greater than 200 m in ship length. All ships present in the image patches were detected. However, some clusters of false alarms comparable to small ships were also detected. The authors of the study stress that the small test set represent a major limitation in the assessment of the proposed method, and that a complete validation on several SAR images presenting different characteristics and environmental conditions is required to establish its suitability in SAR ship detection.

Another method not using the CFAR technique is presented by Tello *et al.* in [15]. The authors of this study are inspired by the human vision operation when dealing with spot detection, and propose a multiresolution time-frequency analysis based on a Wavelet Transform (WT). The method takes advantage of the ships' local statistical behavior in addition to the intensity characteristics of the SAR image. The WT is employed separately in both dimensions (range, azimuth) applying a filter bank. The WT enhances fast changes in the applied direction, thereby increasing the target to clutter ratio. An iterative process named the Over Complete WT (OCWT) is used, producing 3 different outputs per iteration. The 3 outputs are multiplied to get the final product used in the ship detection process. The actual ship detection is done by thresholding. The spatial resolution is preserved in this method, aiding in detection of smaller

vessels. Observed improvement in the target to clutter ratio is reported to be the most noticeable effect of the algorithm.

The proposed method is tested on both single- and dual-polarized detected SAR images. For the dual-pol case, the two channels are multiplied ahead of the OCWT. No direct comparison on ship detection performance for single-polarization vs. dual-polarization is reported, but the target to clutter ratio is shown to be further enhanced going from single-polarization to dual-polarization. Another interesting aspect presented in the study is the fact that the statistical distribution of the clutter is invariant in the wavelet domain, making the algorithm more robust to heterogeneities than conventional CFAR approaches. In addition to this, the algorithm has a reported capability to manage discontinuities, allowing better performance in coastal regions and in the presence of ice.

In [16], Theoharatos *et al.* presents a data fusion technique based on a 2-dimensional principal component analysis (2D-PCA). A CFAR ship detection algorithm based on the Weibull distribution is used, both on the fused product and the individual single-polarization channels. The technique is employed on a RADARSAT-2 quad-pol product (not applicable in this study) and an ENVISAT dual-polarization HH/HV product. Results presented show both increased detection capabilities and a reduction in false alarms.

In [17], Song and Yang presents another ship detection algorithm not relying on the CFAR technique; a so-called tensor robust principle component analysis. The study deals with fully polarimetric SAR products, but can also be applied to single- and multipolarized products. However, the results presented show weaker performance than e.g. the methods described above in [11].

3 Methodology

This chapter starts with an overview of the ship detection software used in the study. Following this, the statistical properties of SAR imagery used in the ship detection process is introduced and evaluated, both for the individual polarization channels and for the combined channels described in 1.4. Then, the data test set forming the base of the analysis is presented. In order to compare the results from the different SAR channels properly, some sort of ground truth is necessary. The chapter ends with a brief presentation of the ground truth application employed.

3.1 Ship detection

The ship detection software used in the study is called Aegir. It is an automatic ship detection tool for SAR imagery developed at FFI [18]. Aegir comes in two different versions; a fully

automatic version and an interactive version in which the operator is able to manage the process from step to step. The different steps in the ship detection process are shown below in Figure 3.1.

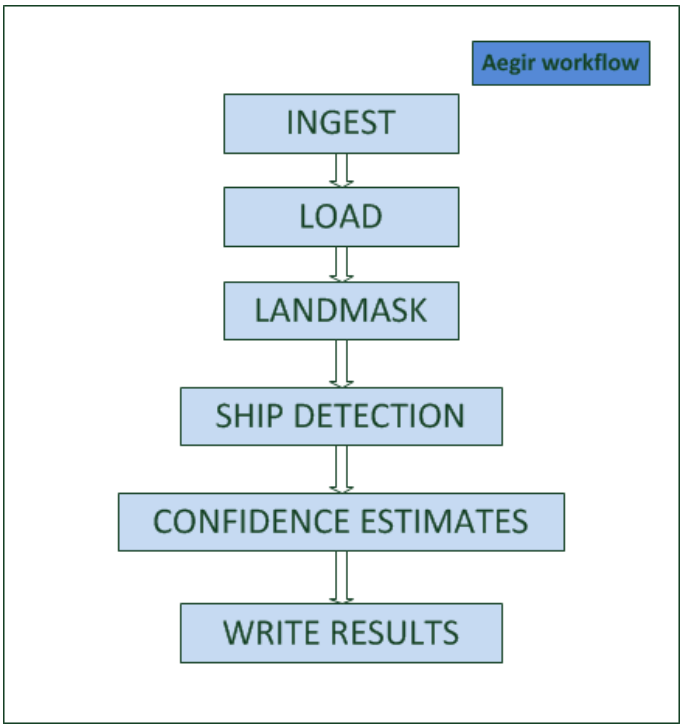

Figure 3.1 Aegir workflow.

The ingest and load steps are merely internal procedures preparing for ship detection. Landmasking is done if necessary. Also, in this step the operator has the option to include a manual mask; this can be advantageous in situation where ice is present. Figure 3.2 shows the main window in the interactive version. The user can control what actions to take by using the buttons on the left hand side. The greater image presents a lower resolution overview image of the entire scene, while the smaller image mirrors the white square in the overview window, only now in full resolution. Note also that the operator can choose what polarization channel to analyze from the menu below the button panel.

The ship detection is done using a sliding window Constant False Alarm Rate (CFAR) approach. This is presented thoroughly by Brekke in a report outlining the use of Aegir [19]. The K-distribution thresholding algorithm is primarily used, but the software also supports the use of the N-sigma algorithm [19].

After ship detection Aegir produces confidence estimates and writes the detection results. The detection result reports include a kml file for plotting in Google Earth and a gml file, used as input to the Multi Hypothesis Tracker (MHT) described below in 3.4.

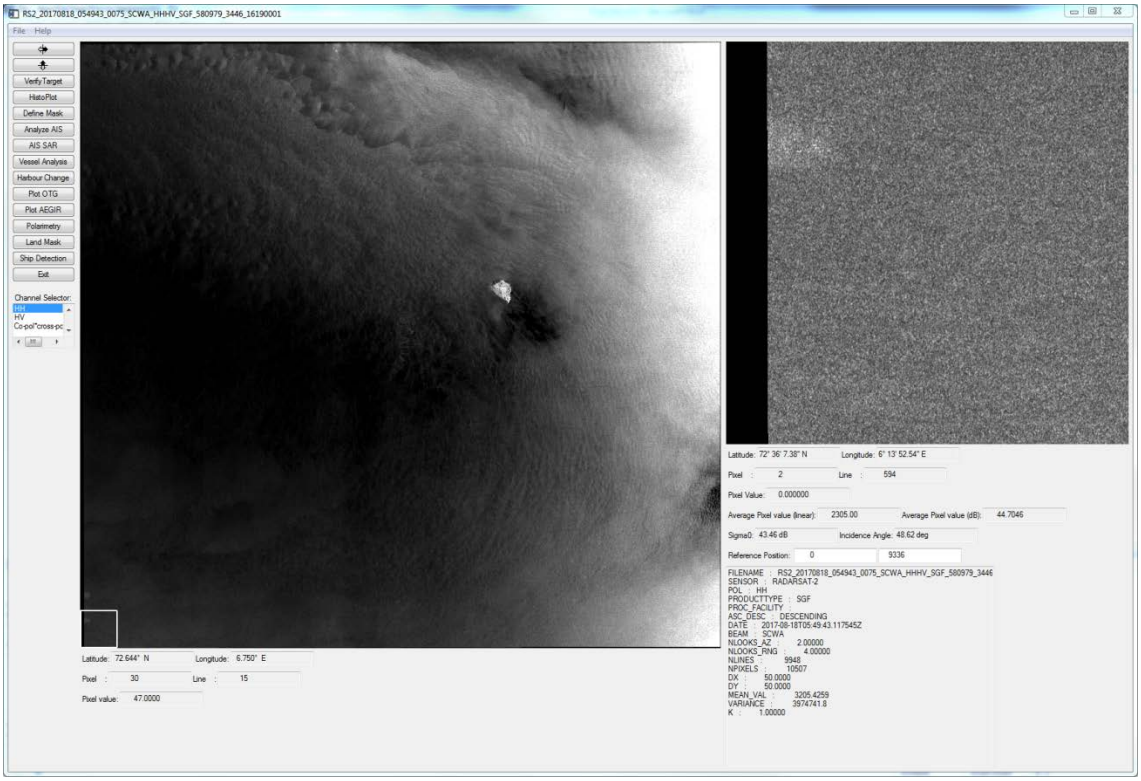

Figure 3.2 Aegir interactive version (RADARSAT-2 August 18th 2017, HH).

3.2 Statistics

Aegir is based on a K-distribution sliding window CFAR ship detection algorithm, see 3.1. For each polarization channel the image is divided into overlapping frames of M pixels x M pixels. In this study, M is set to 100 and the overlap is 20 pixels. As described by Brekke in [19], the K-distribution is widely used in the radar field to represent sea clutter. Equation 3.1 presents the K-distribution.

$$p(x) = \frac{2}{\Gamma(L)\Gamma(\nu)}\left(\frac{L\nu x}{\mu}\right)^{\frac{L+\nu}{2}} K_{L-\nu}\left[2\sqrt{\frac{L\nu x}{\mu}}\right] \tag{3.1}$$

Γ is the gamma function, μ is the mean value of the probability density function (PDF), $K_{L-\nu}$ is the modified Bessel function of the second kind of order L-ν, ν is the order parameter of the PDF and L is the equivalent number of looks (ENL) for the SAR image. The ENL is a measure of the speckle noise, explained by Greidanus and Santamaria in [20]. L and ν are estimated as described in [19]. In order to evaluate the fit of the K-distribution to the actual data, tests have been done on multiple image frames (100 x 100 pixels). Estimates of L and ν, along with a calculated value for μ, provide the necessary information to plot the theoretical PDF, while a

relative histogram has been calculated from the actual data. The histogram bin count was fixed at 1000, leaving the bin size variable by using 0 as the minimum value and the frame maximum pixel value as the maximum value. Examples from testing the statistical fit of the individual polarization channels for RADARSAT-2 are shown in Figure 3.3 and Figure 3.4, for HH and HV, respectively. The horizontal axis shows the pixel value, while the vertical axis shows the probability. The relative histogram count is shown in white, the K-distributed PDF in green. Although the relative histogram count fluctuates to a certain degree, in particular for the HV channel, it is clear that the K-distribution fits nicely with the actual data. The examples are from the RADARSAT-2 image acquired on August 18th 2017 (see 3.3). The Aegir frame number is 8000, meaning the image lines range from 4800 to 4899, while the image pixels range from 6400 to 6499.

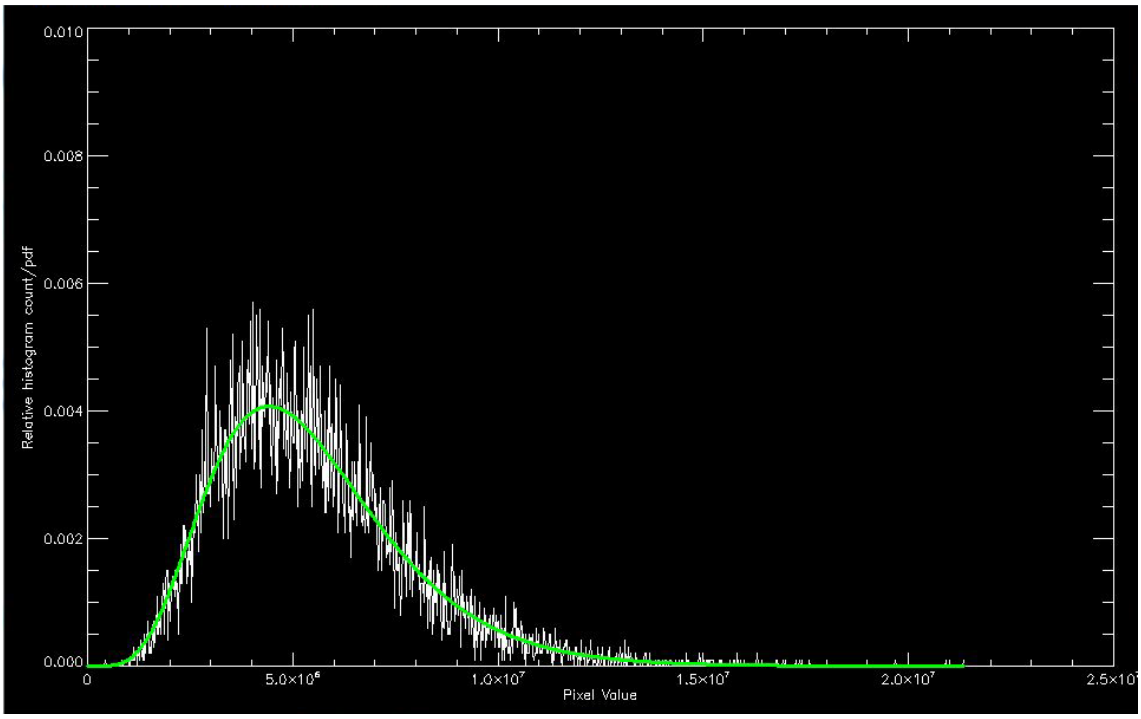

Figure 3.3 RADARSAT-2 August 18th 2017 HH, PDF vs. relative histogram count.

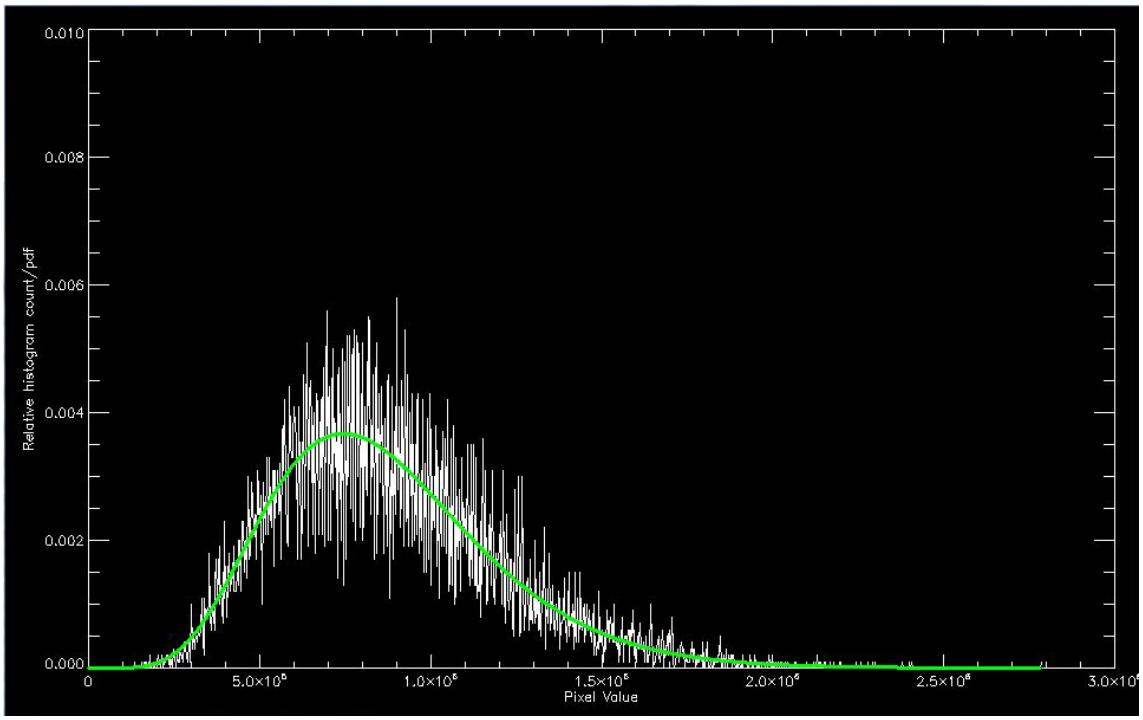

Figure 3.4 RADARSAT-2 August 18th 2017 HV, PDF vs. relative histogram count.

Performing the same exercise for Sentinel-1 images proved a different challenge. The dynamic range was much smaller, and the observed values seemed to be more discretely distributed across the range. In fact, when calculating histograms for the individual polarization channels in the same manner as described above, only 5-12 % of the bins had non-zero values. This made it difficult to estimate the underlying PDF by means of a relative histogram count. However, by assigning interpolated values to the bins with a zero count, and then forcing the new total relative count to 1, a comparison with the theoretical K-distributed PDF was made possible. Figure 3.5 and Figure 3.6 show the interpolated relative histogram count vs. the theoretical K-distributed PDF for individual polarization channels HH and HV, respectively. The examples are taken from the Sentinel-1A image acquired July 17th 2016 (see 3.3). The Aegir frame number is 4742, meaning the image lines range from 2880 to 2979, while the image pixels range from 6400 to 6499.

Obviously, the fit of the theoretical K-distributed PDF to the relative histogram count is not as good as the case is for RADARSAT-2. However, with the aforementioned shortcomings of the Sentinel-1 data when generating a relative histogram count to estimate the true PDF, the fit is reasonably good. Note that for low pixel values, in particular for the co-pol channel, the PDF deviates from the interpolated relative histogram count. This problem will be transferred through to the two combination channels, as they are indeed formed by multiplication, with the co-pol channel as one of the factors.

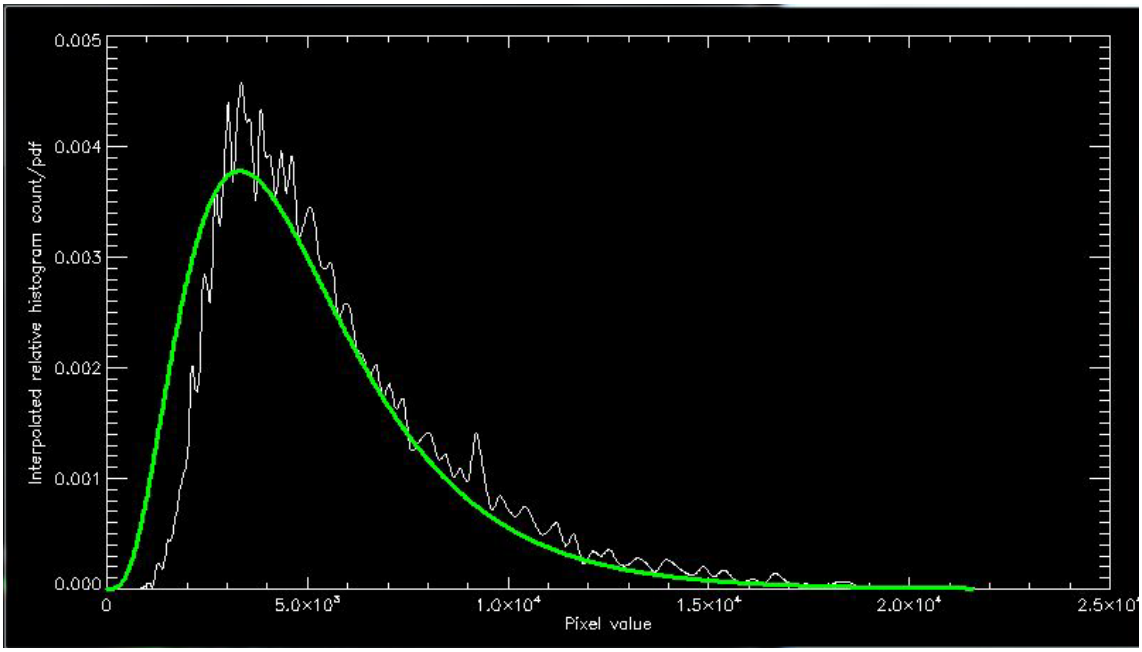

Figure 3.5 Sentinel-1A July 17th 2016 HH, PDF vs. interpolated relative histogram count.

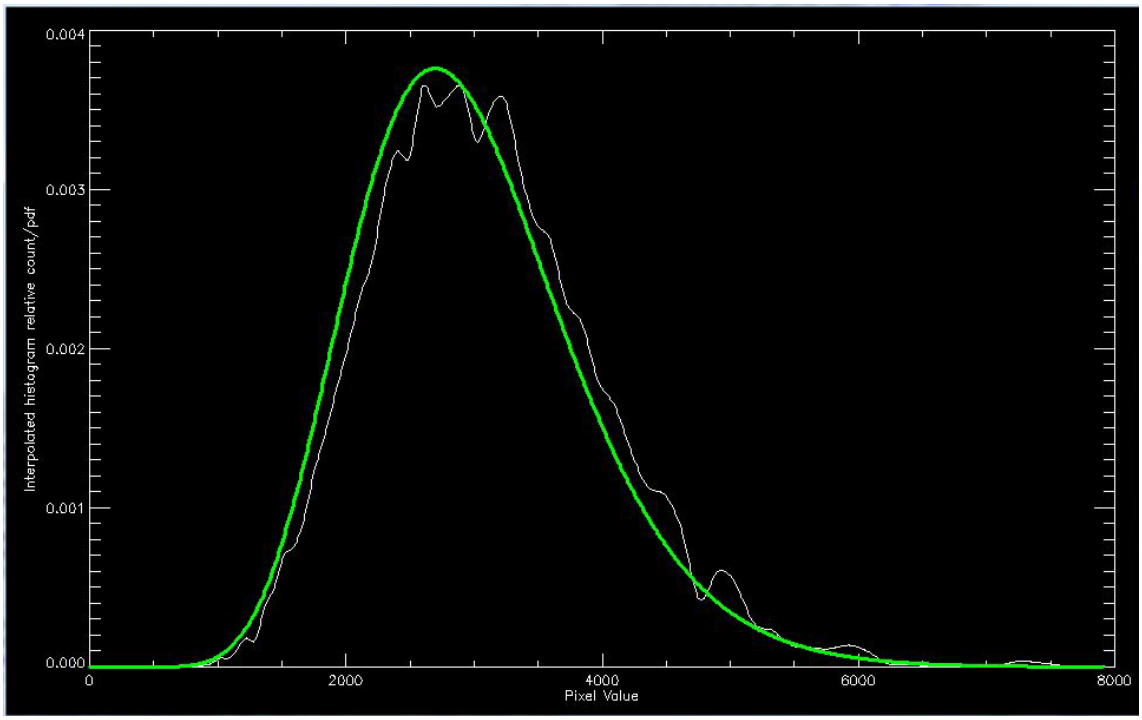

Figure 3.6 Sentinel-1A July 17th 2016 HV, PDF vs. interpolated relative histogram count.

Now, the dual channel is not an ordinary SAR intensity channel, as it is a multiplication of the co-pol and cross-pol amplitude values divided by a constant *C*. When looking at the statistical properties of this channel, the constant *C* can be ignored, as it will not affect the shape of the PDF. Furthermore, as the dual channel is in the intensity domain, the K-distribution has been used to estimate the true PDF of the dual channel in this study. Extensive testing of the fitness of the distribution (same procedure as described above for the individual polarization channels) has been done. Figure 3.7 shows the dual channel estimated K-distribution and the relative histogram for the same frame as shown above for the individual channels for RADARSAT-2. Also now, the PDF fits nicely with the actual data.

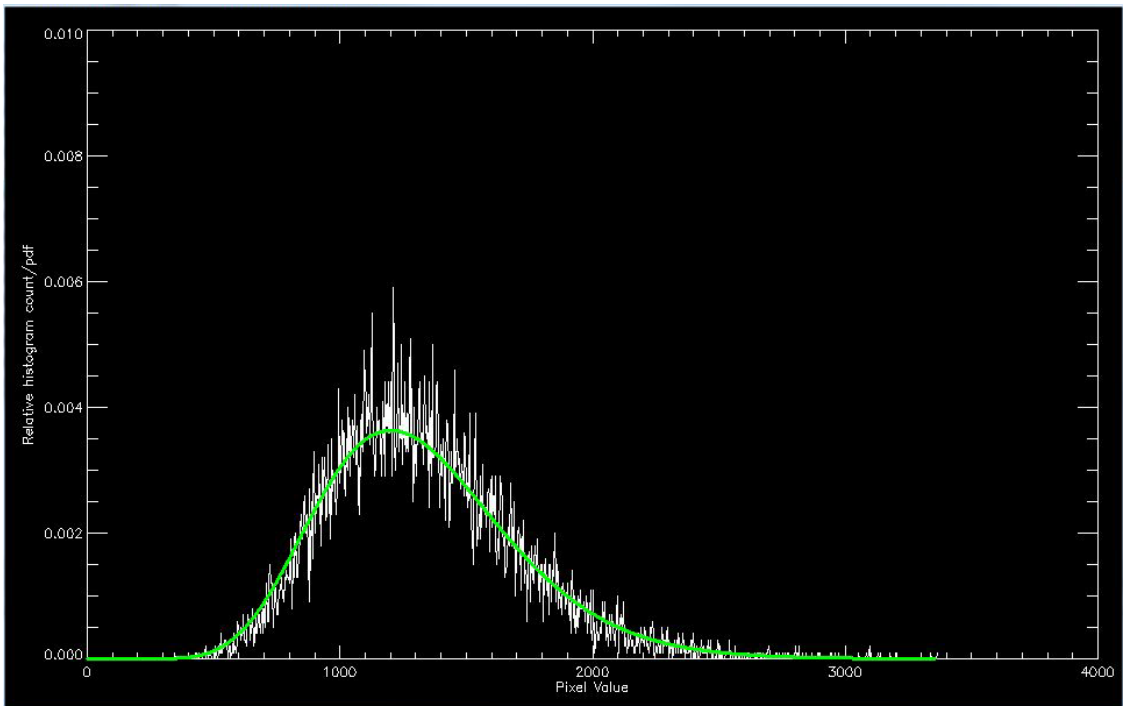

Figure 3.7 RADARSAT-2 August 18th 2017 dual, PDF vs. relative histogram count.

Again, the Sentinel-1 data proved more challenging, but now the non-zero count of the histogram bins was much higher (40 % and above). Also, the zero count bins are all located at low and high end pixel values. Hence, the interpolation and normalization procedure was not used. The relative histogram count for the same frame as above (4742) is plotted along with the estimated K-distributed PDF for the dual pol channel in Figure 3.8. The relative histogram count fluctuates a great deal, but the estimated PDF fits well with the mean value. As noted above, the lack of low pixel values in the co-pol channel affects this comparison; the fit is poorer in the low pixel value area.

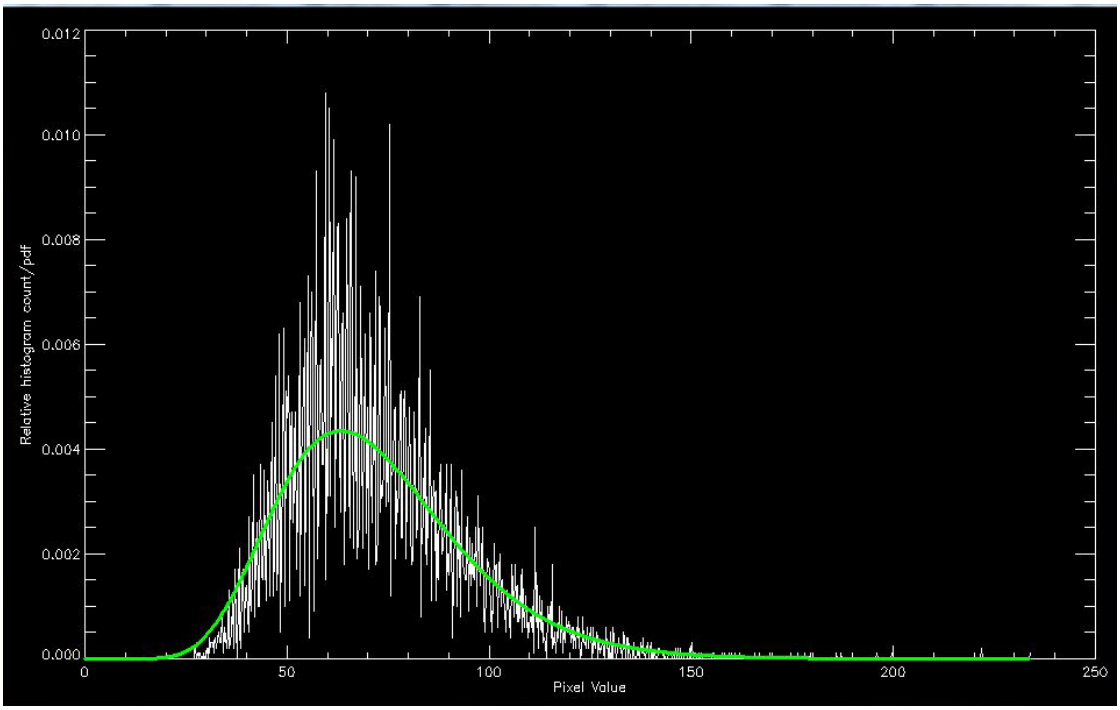

Figure 3.8 Sentinel-1A July 17th 2016 dual, PDF vs. relative histogram count.

The dual-int channel is not in the intensity domain, hence the K-distribution cannot be used. However, noting that the dual-int channel represents a multiplication of two K-distributed channels (co-pol intensity and cross-pol intensity), Knutsen [21] found an expression for the PDF of the dual-int channel, show in equation 3.2.

$$P_U(u) = \frac{1}{u\Gamma(L_1)\Gamma(L_2)\Gamma(\nu_1)\Gamma(\nu_2)} G\begin{matrix}4 & 0\\ 0 & 4\end{matrix}\left(\begin{matrix}- \\ L_1, L_2, \nu_1, \nu_2\end{matrix} \middle| u * \frac{L_1 L_2 \nu_1 \nu_2}{\mu_1 \mu_2}\right) \tag{3.2}$$

Again, Γ is the gamma function. L_1 and L_2 are the ENL for the two individual polarization channels, ν_1 and ν_2 the individual polarization channel's order parameter in the K-distribution, while μ_1 and μ_2 are the mean values. G is the Meijer G-function. See [21] for further details. Note that the expression given in equation 3.2 consists of terms from the individual polarization channels' values for L, ν and μ. Hence, if processing the dual-int channels subsequent to the individual channels, all necessary estimates and calculations are all ready to be used. This reduces the number of calculations needed, hence reducing the processing time. The dual-int channel PDF fit to the actual data has been tested in the same manner as for the individual and dual polarization channels. Shown in Figure 3.9 is the dual-int estimated PDF given by equation 3.2 and the relative histogram for the same frame as shown in Figure 3.3, Figure 3.4 and Figure 3.7. Obviously, the PDF is no longer K-distributed. However, the estimated PDF for the dual-int channel fits nicely with the actual data.

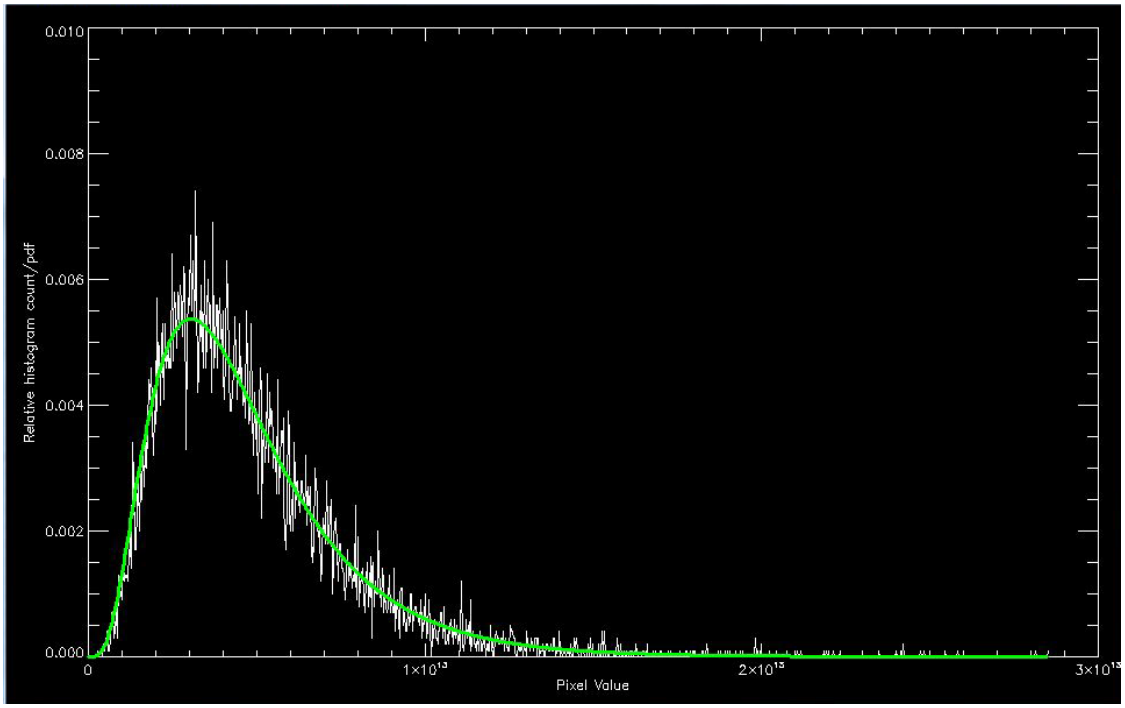

Figure 3.9 RADARSAT-2 August 18th 2017 dual-int, PDF vs. relative histogram count.

The estimated PDF for the dual-int channel vs the relative histogram count for frame 4742 of the Sentinel-1A image acquired July 17th 2016 is shown in Figure 3.10. Also now, the PDF deviates from the actual data for low pixel values. In addition, the central peak of the PDF is a bit too low. For higher pixel values, the estimated PDF fits well with the observed data.

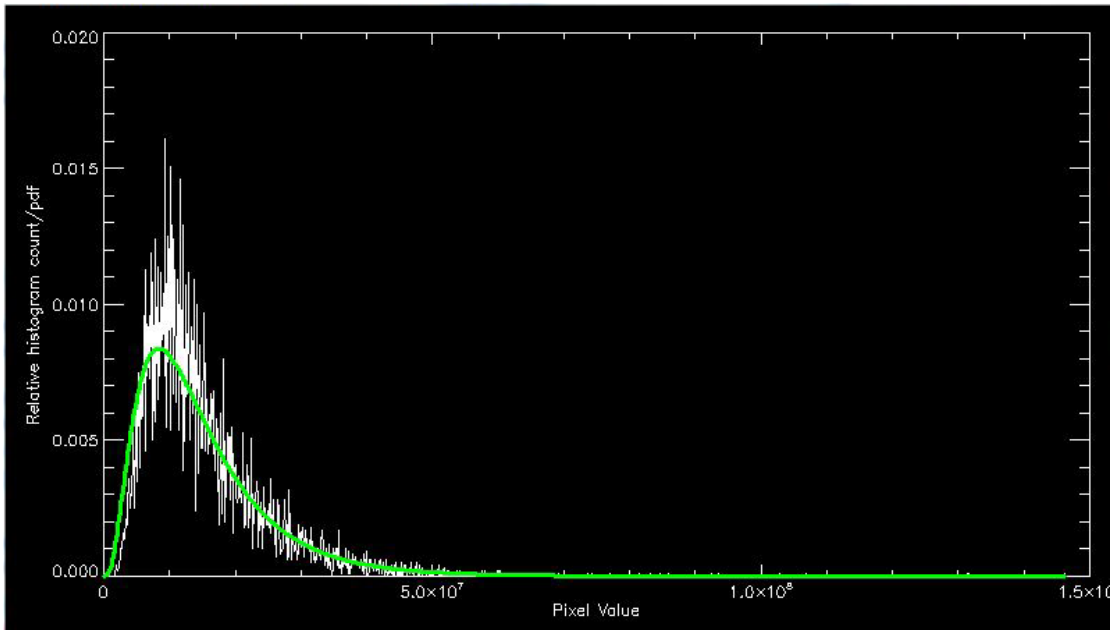

Figure 3.10 Sentinel-1A July 17th 2016 dual-int, PDF vs. relative histogram count.

To sum up, the PDFs used in the ship detection algorithm estimate the actual data well, in particular for RADARSAT-2. For Sentinel-1, the data is less evenly distributed across the range and the proposed PDFs only fit to a certain degree. Note that the goodness of fit has only been evaluated visually, no statistical testing tool such as e.g. the Chi-Square test [22] has been employed. This would certainly have been beneficial in order to get a better understanding of the goodness of fit, but due to time limitations of the study, it was deemed out of scope.

3.3 Data test set

The SAR data set chosen in the study is based heavily on what the Norwegian Armed Forces and the Norwegian Coastal Administration use on a daily basis when monitoring the Norwegian ocean areas. Thus, for RADARSAT-2, only the ScanSAR mode is analyzed. Furthermore, as ScanSAR wide is by far the most used mode, 8 out of 10 RADARSAT-2 products are in this mode. The two remaining RADARSAT-2 scenes are ScanSAR narrow. The choice of polarization also reflects the above mentioned scheme; the RADARSAT-2 test set consists of 9 HH/HV products and 1 VV/VH product. For Sentinel-1, the situation is different, as ESA does not allow for ordering desired products, but bases the acquisition on a so-called High Level Operations Plan (HLOP). Thus, only IW mode in polarization combination VV/VH and EW mode in polarization combination HH/HV are available in Norwegian waters. Hence, the data set chosen for the Sentinel-1 platform are split evenly between the available modes; 5 IW and 5 EW. All products but one is medium resolution, as this is the product type used mostly. The single high resolution product analyzed was included for completeness. The geographical locations of the data sets are shown in Figure 3.11 for RADARSAT-2 and Figure 3.12 for Sentinel-1.

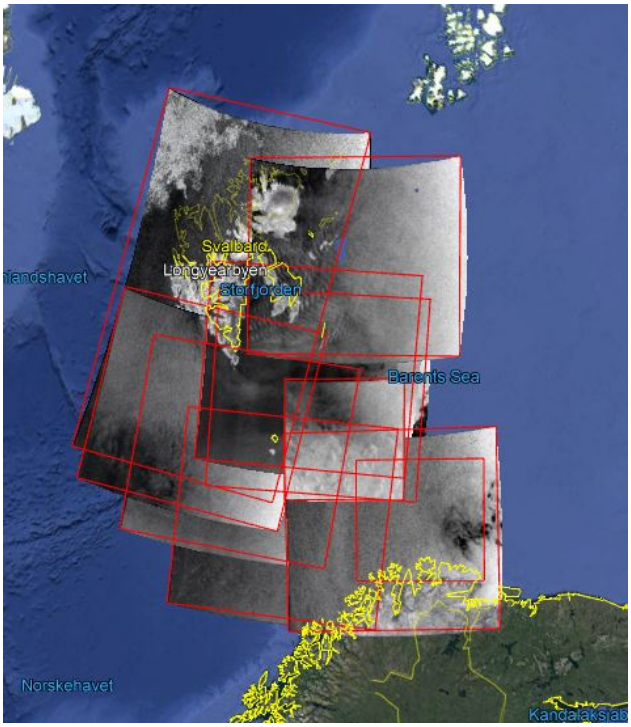

Figure 3.11 RADARSAT-2 data set geographical location.

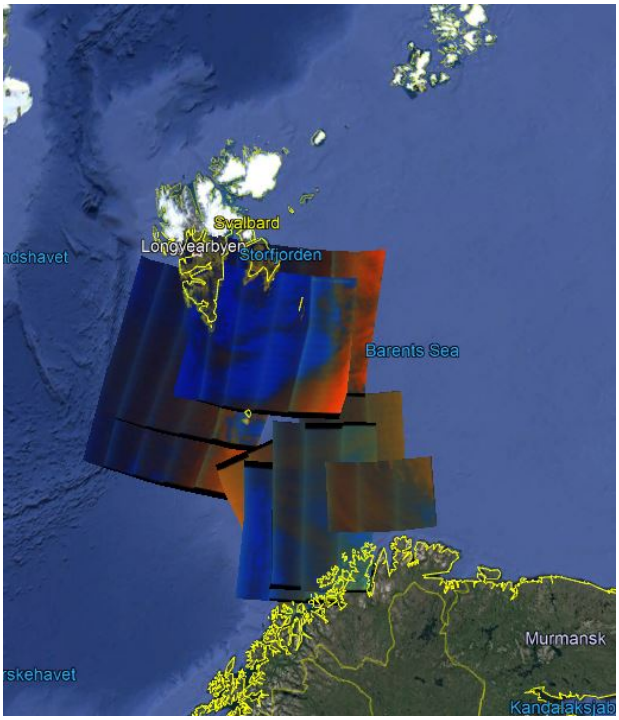

Figure 3.12 Sentinel-1 data set geographical location.

Table 3.1 and Table 3.2 show the details of the data sets, split by platform. In Table 3.2, S1A refers to Sentinel-1A, while S1B refers to Sentinel-1B.

Table 3.1 RADARSAT-2 data test set.

Test ID #	Date	Mode	Polarization
1	20160125	ScanSAR Narrow	HH/HV
2	20160717	ScanSAR Wide	HH/HV
3	20160724	ScanSAR Wide	HH/HV
4	20170502	ScanSAR Wide	HH/HV
5	20170603	ScanSAR Wide	HH/HV
6	20170818	ScanSAR Wide	HH/HV
7	20170915	ScanSAR Wide	HH/HV
8	20170924	ScanSAR Wide	HH/HV
9	20170926	ScanSAR Wide	HH/HV
10	20171027	ScanSAR Narrow	VV/VH

Table 3.2 Sentinel-1 data test set.

Test ID #	Date	Platform	Mode	Resolution	Polarization
11	20160125	S1A	IW	H	VV/VH
12	20170517	S1A	IW	M	VV/VH
13	20170907	S1A	IW	M	VV/VH
14	20171106	S1B	IW	M	VV/VH
15	20171114	S1B	IW	M	VV/VH
16	20160717	S1A	EW	M	HH/HV
17	20170627	S1B	EW	M	HH/HV
18	20170629	S1B	EW	M	HH/HV
19	20170727	S1A	EW	M	HH/HV
20	20170830	S1B	EW	M	HH/HV

Looking at the date column of the data test sets, an attempt was made to include SAR imagery from different parts of the year. This was done to test the combined channels in different environmental conditions. For instance, images with ice present have been processed as is (no ice mask) in order to determine the performance of the channels in such challenging conditions.

3.4 Ground truth

In order to compare the performance of the different channels, both in terms of true detections and false alarms, some sort of ground truth is necessary. A Multi Hypothesis Tracker (MHT),

also developed at FFI, has been used in this study for ground truth. The MHT employs multiple cooperative positioning data to track ships and identify detections from SAR images accurately [23]:

- Vessel Monitoring System (VMS)
- Long Range Identification and Tracking (LRIT)
- Automatic Identification System (AIS), both terrestrial and satellite receivers

The MHT identifies detections in SAR imagery by including them in the different hypothesis when generating ship tracks. It's important to realize that the MHT does not offer a complete ground truth, as some vessel may not be tracked properly. This can be due to e.g. difficulty of tracking in congested areas, lack of cooperative data due to coverage gaps or system downtime, or that some ships do not transmit positional data at all. The latter may or may not be intentional, but tracking them by means of cooperative data is nevertheless impossible. False alarm detections will most probably not be tracked, as the reported ship detection does not stem from an actual ship. In addition to this, the ship detection software may detect some vessels more than once as a result of vessel shape and backscatter characteristics. In this situation, the MHT will at most identify one of the detections, as the other(s) are indeed false alarms.

With the above in mind, the ground truth provided by MHT is not perfect, but it is nevertheless an excellent tool to get as close as possible to the ground truth without employing costly measures such as e.g. surveillance planes. Thus, any detection identified by MHT in this study has been labelled a true detection. On the other hand, any detection not identified by MHT has been labelled a false alarm.

4 Results and analysis

This chapter starts off by comparing the different channels in terms of identified detection performance. Hence, only the detections identified by MHT will be treated. The CFAR ship detection algorithm was run with P_{FA} set to 10^{-8} for all test cases. Following this, a false alarm analysis is presented, including both a count of the observed false alarms and a closer look at some of the reasons behind. Finally, the detection confidence estimate procedure used in Aegir is presented and evaluated.

4.1 Identified detections

In order to evaluate the performance of the combined channels, the number of identified detections is of prime importance. In addition to this, pooling the results from the individual polarization channels and the combination channels will provide a measurement of the added value provided. In the following, the dual combination and the dual-int combination channels are treated separately, as they are similar in nature and the main aim is to compare the results from these two channels with the individual polarization channels. Table 4.1 and Table 4.2 present the ship detection results in terms of identified detections for the individual polarization channels, and the dual and dual-int combination channels, respectively. The column headers, from left to right, are: Test case ID number, polarization combination, total number of identified detections across the four channels, co-pol channel (HH or VV), cross-pol channel (HV or VH), dual or dual-int channel, co-pol and cross-pol pooled, co-pol and dual (-int) pooled, cross-pol and dual (-int) pooled and finally co-pol, cross-pol and dual (-int) pooled. For each test case, the channel(s) or union(s) with the best result is shown with a green background, except for the union of all three channels which is only shown with a green background if it contains the best result exclusively. This is done to highlight the fact that pooling all three channels will always have the best result, but both the individual channels and/or unions thereof may perform equally well.

Table 4.1 Identified detection count co-pol, cross-pol, dual and their unions.

ID #	Pol	Total	CO	CX	D	CO U CX	CO U D	CX U D	CO U CX U D
1	HH/HV	44	16	38	40	40	40	42	42
2	HH/HV	14	12	12	14	14	14	14	14
3	HH/HV	40	27	34	36	40	37	39	40
4	HH/HV	31	21	28	30	30	30	31	31
5	HH/HV	30	6	29	23	30	23	30	30
6	HH/HV	38	17	35	35	35	35	38	38
7	HH/HV	32	17	29	28	31	29	31	32
8	HH/HV	37	8	33	34	34	34	37	37
9	HH/HV	34	23	29	32	32	32	33	33
10	VV/VH	9	8	9	9	9	9	9	9

ID #	Pol	Total	CO	CX	D	CO U CX	CO U D	CX U D	CO U CX U D
11	VV/VH	35	30	35	34	35	34	35	35
12	VV/VH	26	26	24	25	26	26	25	26
13	VV/VH	23	22	20	17	23	22	20	23
14	VV/VH	18	14	16	16	18	16	18	18
15	VV/VH	11	10	10	10	11	11	10	11
16	HH/HV	10	10	8	10	10	10	10	10
17	HH/HV	8	3	8	7	8	7	8	8
18	HH/HV	17	7	16	17	16	17	17	17
19	HH/HV	13	13	10	12	13	13	12	13
20	HH/HV	26	20	25	24	26	26	25	26

From a first inspection of the results in Table 4.1, it makes sense to treat the RADARSAT-2 (IDs 1-10) and Sentinel-1 (IDs 11-20) test cases separately. For RADARSAT-2, the dual combination channel consistently performs better than the co-pol channel, while the performance is equal to or better than the cross-pol channel in 8 out of 10 test cases. Furthermore, looking at the different pooled combinations, the dual combination channel offers improved performance in 6 of the 10 investigated scenes. The increase in number of identified detections ranges from 1 to 3, but it is nevertheless an improvement. Pooling the dual combination channel with the cross-pol channel, the result reaches the top mark in 8 out of 10 test cases. Only test case 3 shows the best performance without including the dual combination channel, while test case 7 is the only test case where all three channels are included in the highest identified detection count.

For the Sentinel-1 test cases, the story is quite different. Now, the dual combination channel performs equal to or better than the co-pol channel in 7 out of 10 test cases. The corresponding number when comparing the dual combination channel with the cross-pol channel is 6 out of 10 cases. However, looking at the pooled combinations, the dual combination channel now offers increased performance in a single test case only (18). Pooling the co-pol and the cross-pol channels achieves the highest count of identified detections for the remaining nine test cases. Note that none of the test cases now require all three channels to be included on order to reach the highest identified detection count.

Comparing the total number of identified detections with the pooling of the co-pol, cross-pol and dual combination channels in the rightmost column, the latter matches the total count in 18 out of 20 cases. For test case 1, the pooled number of detections from all three channels is 42 while the total number of identified detections is 44. For test case 9, the corresponding numbers are 33 and 34. This simply means that the dual-int combination channel, which results are detailed in the next paragraph, has identified detections not included in the dual-combination channel results for these two test cases.

Table 4.2 Identified detection count co-pol, cross-pol, dual-int and their unions.

ID #	Pol	Total	CO	CX	D-I	CO U CX	CO U D-I	CX U D-I	CO U CX U D-I
1	HH/HV	44	16	38	43	40	43	44	44
2	HH/HV	14	12	12	14	14	14	14	14
3	HH/HV	40	27	34	37	40	38	39	40
4	HH/HV	31	19	28	30	30	30	31	31
5	HH/HV	30	6	29	22	30	22	30	30
6	HH/HV	38	17	35	34	35	35	38	38
7	HH/HV	32	17	29	28	31	29	31	32
8	HH/HV	37	8	33	25	34	26	34	35
9	HH/HV	34	23	29	23	32	29	33	34
10	VV/VH	9	8	9	9	9	9	9	9
11	VV/VH	35	30	35	35	35	35	35	35
12	VV/VH	26	26	24	25	26	26	25	26
13	VV/VH	23	22	20	17	23	22	20	23
14	VV/VH	18	14	16	12	18	15	16	18
15	VV/VH	11	10	10	9	11	11	10	11
16	HH/HV	10	10	8	10	10	10	10	10
17	HH/HV	8	3	8	7	8	7	8	8
18	HH/HV	17	7	16	17	16	17	17	17
19	HH/HV	13	13	10	12	13	13	13	13
20	HH/HV	26	20	25	21	26	25	25	26

Now, looking at the results including the dual-int combination channel in Table 4.2, the main trends agree with the dual combination results. For RADARSAT-2, the dual-int combination channel consistently outperforms the co-pol channel, while it performs equal to or better than the cross-pol channel in 5 out of the 10 test cases. Again, looking at the different pooled combinations, including the dual-int combination channel leads to an increase in performance in 6 out of 10 test cases. However, now only 6 of the pooled cross-pol and dual-int reports performance at the high mark, as the highest identified detection count when pooling co-pol, cross-pol and dual-int has risen to 3. As for the dual combination channel, only test case 3 shows the best performance when not including the dual-int combination channel.

For Sentinel-1, the dual-int combination channel performs equal to or better than the co-pol channel in 5 of 10 test cases, a slight drop compared to the dual combination channel. This is also the case when comparing the dual-int combination channel with the cross-pol channel; the identified detection count is equal or better in 4 of 10 test cases. Once again, only test case 18 is seeing an improvement in performance from the inclusion of the dual-int combination channel when looking at the different pooled combinations. The pooled co-pol and cross-pol results also now achieve the highest count in identified detections for 9 test cases.

Test case 8 is now the only case where the co-pol, cross-pol and dual-int combination channels pooled count is lower than the total count; 35 versus the total count of 37. As explained in the previous paragraph, this means that the dual combination channel has two identified detections not found in the dual-int combination channel for this test case.

In order to get a better picture of how the two presented dual polarization combination channels perform with respect to each other, Figure 4.1 shows the number of identified detections per channel for the 20 test cases. The dual combination channel is labelled D and shown in green, while the dual-int combination channel is labelled D-I and shown in purple. Generally, the two channels perform at the same level, but the dual combination channel has a few more identified detections. This is most evident for test cases 8 and 9. The total count of identified detections for the dual combination channel is 453, while the total count for the dual-int combination channel is 430. Hence, for the 20 test cases analyzed in this study, the dual combination channel is the better one in terms of number of identified detections. For completeness, the total counts for the co-pol and cross-pol channels are 306 and 448, respectively.

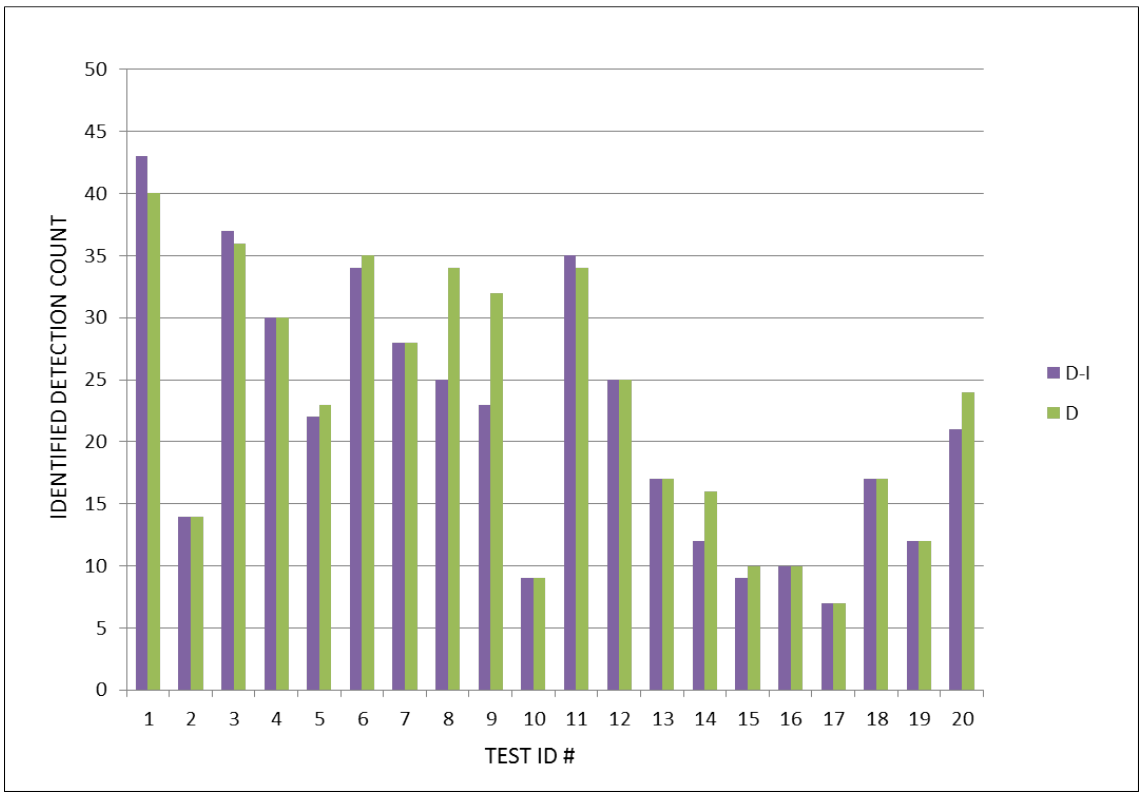

Figure 4.1 Identified detections dual vs. dual-int combination channels.

4.2 False alarms

False alarms, i.e. detections done by the automatic ship detection tool that proved not to be ships (in this study; detections not identified by MHT), plays another important role in evaluating the

performance of the ship detection algorithm. Table 4.3 shows the number of false alarms for the SAR images analyzed in this study. The column headers are defined as in Table 4.1 and Table 4.2. Obviously, some of the images have a very high false alarm count. In the following, three different reasons for high false alarm counts are examined closer, and the test cases applicable to these reasons are determined.

Table 4.3 False alarm count.

ID #	Pol	CO	CX	D	D-I
1	HH/HV	8	11	7	13
2	HH/HV	26	5	3	8
3	HH/HV	355	5	72	230
4	HH/HV	46	21	22	32
5	HH/HV	205	50	104	443
6	HH/HV	1	6	8	8
7	HH/HV	7	8	7	13
8	HH/HV	167	30	88	415
9	HH/HV	12	10	14	5
10	VV/VH	0	1	1	4
11	VV/VH	12	12	13	11
12	VV/VH	62	8	2	2
13	VV/VH	136	3	10	5
14	VV/VH	0	0	0	0
15	VV/VH	0	5	0	0
16	HH/HV	51	2	19	39
17	HH/HV	3	4	4	3
18	HH/HV	5	20	33	26
19	HH/HV	181	8	35	72
20	HH/HV	4	8	3	1

Test ID 13, the Sentinel-1A IW VV/VH medium resolution product acquired September 7th 2017 has a high number of false alarms in the co-pol channel (VV). Figure 4.2 shows a screenshot from Aegir with detections in VV, VH and dual shown in purple, yellow and green diamonds, respectively. Detections in dual-int are not shown. Note that the images is flipped both north-south and east-west, this is due to the read-in process in Aegir. The zoomed-in image on the right hand side (VV) provides insight into the main reason for the high false alarm count. In low wind conditions these patterns can often occur in the co-pol channel. They form due to algae growth [24] and are the reason for the high number of false alarms. The patterns also occur in the dual and dual-int channels, but are not nearly as strong. Thus, as can be seen in

Table 4.3, these two channels do not have corresponding high counts. The phenomenon described here also applies for test ID 12. Hence, it seems that low wind conditions, causing high numbers of false alarms in VV, does not transfer to the two combination channels investigated in this study.

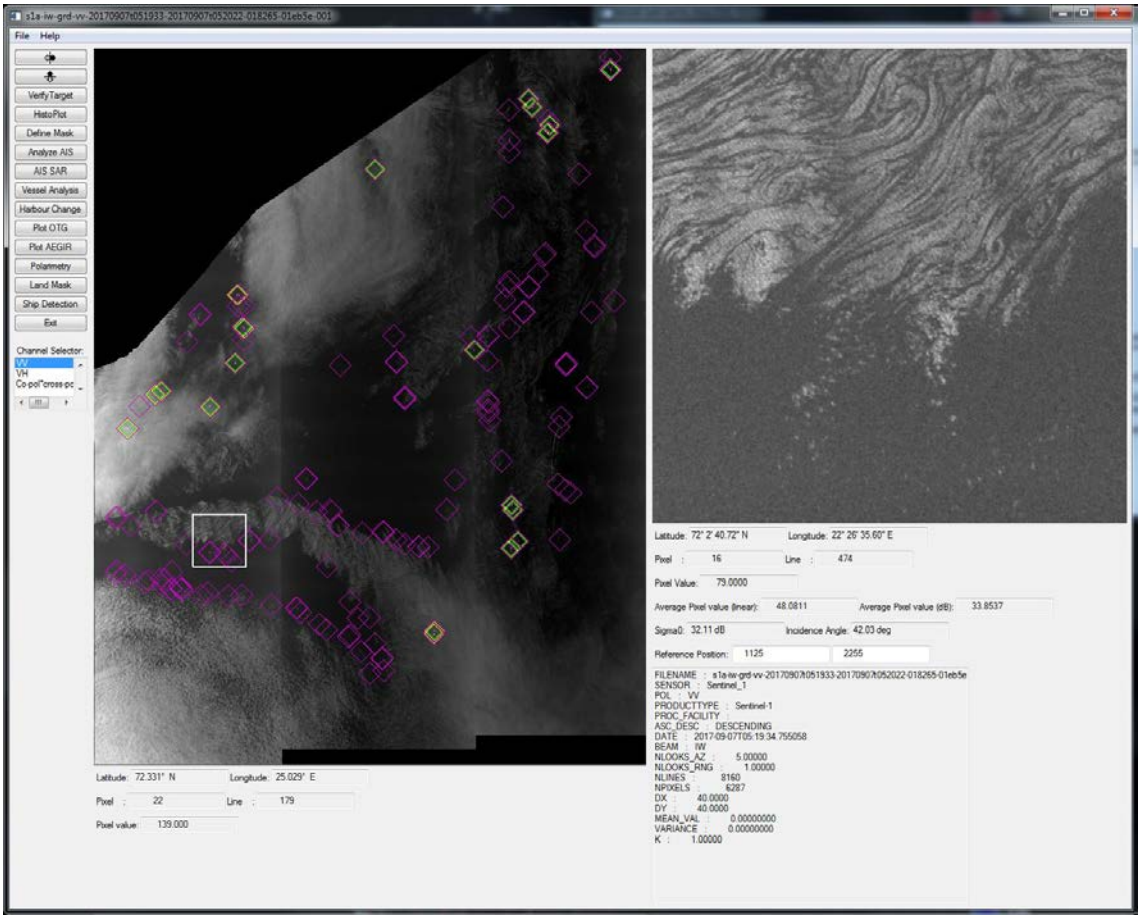

Figure 4.2 False alarms, Sentinel-1A September 7th 2017.

As described in Section 3.3, images containing ice were deliberately included in the test set in order to determine if the combination channels deal differently with this issue compared with the co- and cross-pol channels. Figure 4.3 shows a good example of ice causing false alarms. Shown here is the co-pol channel (HH) of test ID 5, a RADARSAT-2 ScanSAR Wide scene acquired June 3rd 2017. Detections in HH, HV and dual are shown in purple, yellow and green diamonds, respectively. Detections in dual-int are not shown. Note that the image is flipped north-south. The big ice belt stretching from Svalbard down to Bear Island causes a lot of false detections. The dual channel handles the ice better than the co-pol channel, while the dual-int channel handles it worse. The cross-pol channel is the best performing channel in terms of the lowest number of false alarms. Test IDs 8, 18 and to a lesser degree 9, also contains plenty of ice. Results from test ID 8 follows the same pattern as shown for test ID 5, while test ID 18 has fewer false alarms in co-pol. Nevertheless, the dual channels, in particular the dual-int channel,

perform far worse than cross-pol. Generally, the combination channels do not seem to deal very well with ice.

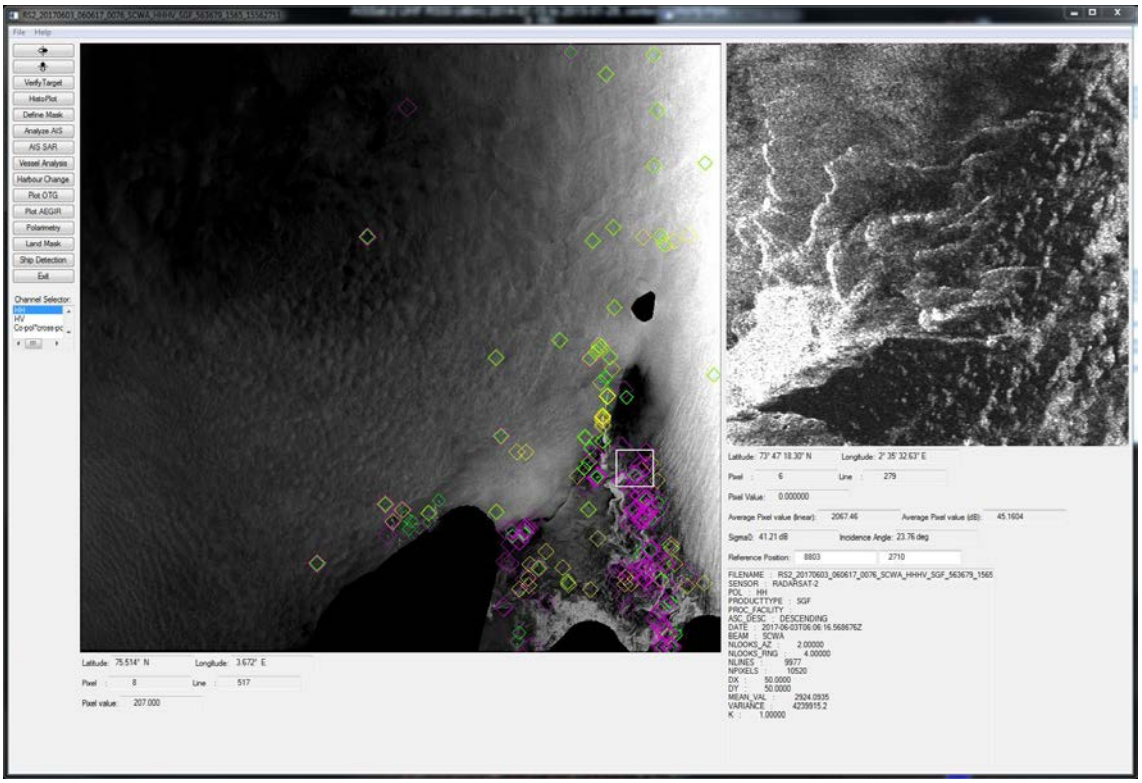

Figure 4.3 False alarms, RADARSAT-2 June 3rd 2017.

Figure 4.4 presents the third major cause of false alarms seen in this study; detections in co-pol at low incidence angles. The screenshot from Aegir is from test ID 3, the RADARSAT-2 scene acquired July 24th 2016. Also now, the image is flipped north-south. Detections from HH, HV and dual are shown in purple, yellow and green diamonds, respectively. Detections in dual-int are not shown. From Table 4.3 it is clear that the dual-int channel performs better than the co-pol channel, even though the false alarm count is still very high. The dual channel has fewer false alarms than the dual-int channel, but the count is still high. Test ID 19 follows the same pattern with a high count of false alarms in co-pol, dual and dual-int, all located at low incidence angles. Hence, the known problem of frequent occurrences of false alarms at low incidence angles for co-pol seems to persist in the dual combination channels presented in this study. However, as will be explained in more detail in 4.3, the confidence estimate procedure applied in Aegir could be used to disregard these detections, or at least label them with a low confidence.

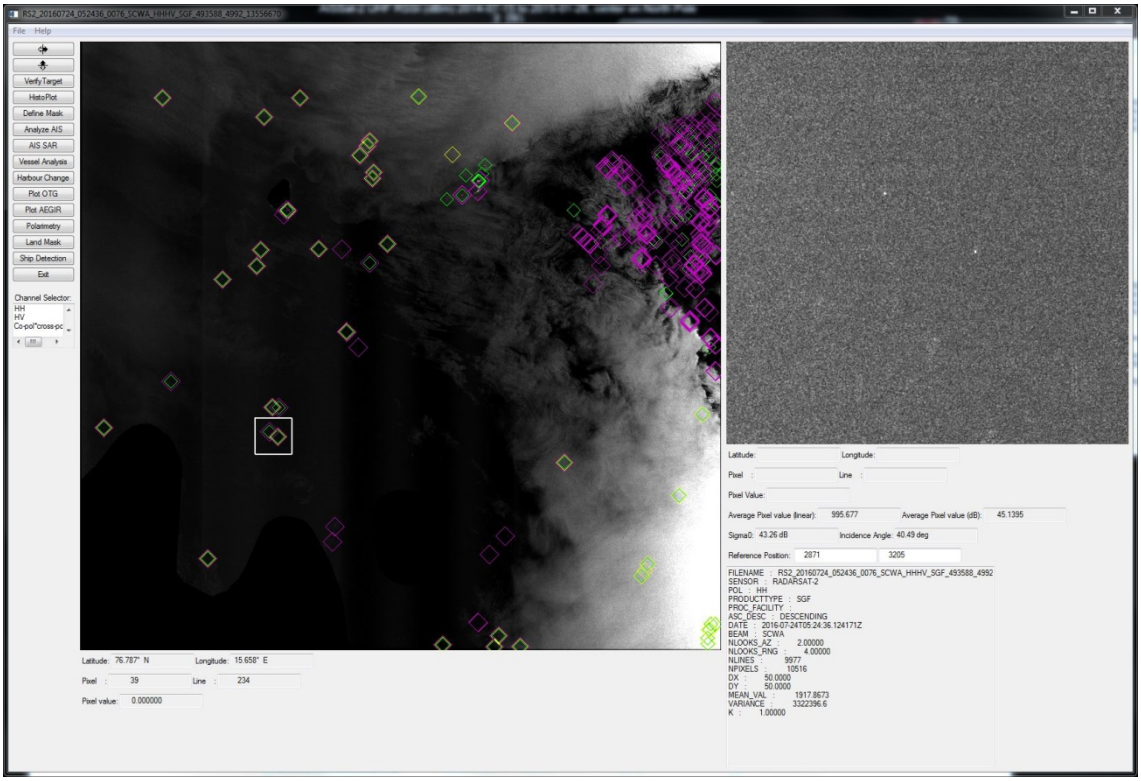

Figure 4.4 False alarms, RADARSAT-2 July 24th 2016.

In addition to the three causes for false alarms described above, double detection of single target and SAR processing problems causing artefacts in the image account for some of the false alarms (e.g. test case 16), particularly in the cross-pol channel. Also, it's important to keep in mind that the MHT, as described in 3.4, does not offer a complete ground truth. Hence, some of the detections that have been labelled as false targets may actually be good detections.

4.3 Confidence estimates

Aegir produces a confidence estimate (CE) for each ship detection candidate. The algorithm used is described thoroughly by Hannevik and Olsen in [25]. To give a brief summary, an initial CE is calculated based on ship size, ship-to-sea-contrast, morphology and ship wake. Note that for RADARSAT-2 ScanSAR products, few wakes are observed; hence this factor is set to zero. In this study, this also applies to the Sentinel-1 products. Subsequent to the initial estimate, the CE is adjusted based on incidence angle and the number of channels it has been detected in. Based on experience with operational users, the CE is then simplified by associating an integer value between 0 and 3, where 0 is *not a ship* and 3 is *certain ship*.

The initial CE depends heavily on the estimated ship size (the morphology is calculated as the ship width to length fraction). However, the reported ship dimensions seen in this study suggests that the algorithm used to estimate the dimensions is unstable. Some detections are reported with plausible dimensions, while others are reported with very unlikely lengths and

widths. This makes the CE unreliable even before the adjustment for incidence angle and detection in several channels. Thus the CE has not been used actively in this study. A good example of how the CE could have been used to reduce false alarms is shown above in Figure 4.4, where HH reported many false alarms at low incidence angles. In fact, all these detections have a CE set to 0 (not ship), and could thus have been left out of the reported ship detections. Nevertheless, due to the instability of the dimension estimates, the CE algorithm was left as is, and no analysis of the impact of the dual pol channels have been made. This being said, detections made in the dual pol channels could have been used in the CE adjustment described above (detection in more than one channel). However, altering the CE algorithm has been considered out of scope for this study.

5 Discussion

Two SAR dual polarization combination channels have been analyzed for use in automatic ship detection. The first channel, called dual, is the product of the individual polarization channel amplitudes, scaled by a calculated average sea background. The second channel, called dual-int, is the product of the individual polarization channel intensities. Ship detection results from both combination channels have undergone both a qualitative and quantitative analysis.

The results presented show that the added value of introducing a combination channel differs between the two SAR platforms used. When analyzing ship detection results using RADARSAT-2 imagery, both dual polarization combination channels generally offer added value in terms of increased numbers of identified detections. This is generally not the case for Sentinel-1 imagery. The reasons for this are unclear, but the difference in statistical properties may at least partially explain the difference in performance. The two dual combination channels were presented as a method of increasing the ship-to-sea (target-to-clutter) ratio, thus making it easier to separate pixels belonging to ships from pixels belonging to the sea clutter. Commonly used in SAR ship detection, the individual polarization channel sea clutter intensity was expected to follow a K-distribution. In chapter 3.2, actual SAR data was compared with the estimated K-distributed PDF belonging to the same image frames. It was evident that RADARSAT-2 data is well modelled by the K-distribution, both for co-pol and cross-pol data. However, this was not clear for Sentinel-1 data. Furthermore, the presented dual combination channels also assume the individual polarization channel sea clutter intensity to follow a K-distribution. Again, both channel combinations were shown to fit nicely with the actual data for RADARSAT-2. Unsurprisingly, the fitness of the theoretical PDF was not as good for Sentinel-1. It may be that the shortcomings of the statistical fit seen in the individual polarization channels are emphasized in the dual combination channels, thereby affecting the performance in a negative manner. This being said, both dual combination channels generally performed at the same level as the individual polarization channels, but did not provide added value in terms of increased number of identified detections. Based on this, it is recommended to study the

statistics of the Sentinel-1 data in a more in-depth manner than what was possible within the time limits of this study.

Comparing the ship detection result from the two presented dual polarization combination channels with the individual polarization channels, both dual and dual-int generally outperforms the co-pol channel, at least for co-pol with HH polarization. For co-pol with VV polarization, the results are more varying, suggesting less gain in introducing the combination channels when working with VV/VH products. Now, the two dual combination channels generally perform at the same level as the cross-pol channel, independent of the polarization. This being said, the dual combination channels do not necessarily detect the same vessels as the cross-pol channel, but the number of identified detections are similar. Furthermore, as discussed in the previous paragraph, the dual combination channels seem to offer additional information in terms of ships not detected in the individual polarization channels for RADARSAT-2 imagery. This is however not the case for Sentinel-1 imagery, leading to the conclusion that based on the test cases investigated in this study, the dual combination channels generally both add value in terms of unique ship detection for RADARSAT-2, but not for Sentinel-1.

False alarms represent a common problem in SAR ship detection. Subsets of the test cases chosen for this study were selected in order to investigate well known problematic phenomenon causing false alarms, especially in the co-pol channels. Under very low wind condition, patterns emerging from algae growth present difficult conditions for automatic ship detection. As described above for test cases 12 and 13, the presented dual combination channels do not seem to suffer from this phenomenon, outputting far fewer false alarms compared to the co-pol channel. Ice represents a second well known problem, not only for the co-pol channel, but for the cross-pol channels as well. Results in this study generally show that the dual combination channel handles ice better than the co-pol channel. On the other hand, the dual-int combination channel generally performs worse than the co-pol channel. The cross-pol channel generally performs best in terms of the lowest false alarm count in ice-infested waters. The third problem deals with false alarms counts at low incidence angles in co-pol. Both dual combination channels outputs fewer false alarms compared with the results from co-pol. Between the two combination channels, the dual channel performs better. However, the numbers are still high compared with the cross-pol channel. To sum up, the dual combination channel deals with known phenomenon causing false alarms better than the dual-int channel, but is still generally outperformed by the cross-pol channel.

Now, having evaluated the performance of the presented dual combination channels, how can the additional information provided be utilized in the best possible manner? For RADARSAT-2, the dual channels generally increase the overall number of identified detections. Thus, the combination channels offers information beyond what was provided by the individual polarization channels. This is, as stated above, not the case for Sentinel-1 data. However, the detections from the dual combination channels can still be used in the confidence estimate procedure. Of course, this is also the case for RADARSAT-2. Unfortunately, the confidence estimates provided by Aegir in this study were determined unreliable, mainly due to the unstable performance of the ship detection dimension analysis. Also, an in-depth study of the

reasons leading to this instability has been deemed out of scope due to time limitations. However, the additional information provided by the dual combination channels can of course be used in an updated confidence estimate procedure in Aegir. In particular, the detection of a target in multiple polarization channels already increases the confidence estimate. Adding the dual polarization combination channels to this part of the procedure could be implemented in the same way as is currently being done for the individual polarization channels.

Time is more than often a factor when working with maritime surveillance, in particular in an operational context. The time between image acquisition and reported ship detections is thus of great importance. The two dual polarization channels presented in this study differ slightly in the number of required operations, based on the statistical modelling presented in 3.2. When doing ship detection in the dual channel, the PDF order parameter and mean value will have to be calculated for every frame, as for the individual polarization channels. The dual-int channel uses the order parameters and mean values from the individual polarization channels, and thus the number of required operations involved in the detection algorithm is lower. Although a timing analysis has not been done in this study, with the current speed of computers, the advantage of the dual-int channel in terms of fewer operations is not believed to be great. However, if time is crucial, the results presented in this study suggests only processing the cross-pol and dual combination channel for RADARSAT-2, while only processing the co-pol and cross-pol channel for Sentinel-1.

To sum up, two dual polarization combination channels for use in SAR ship detection have been presented, named dual and dual-int. The dual combination channel generally performs better than the dual-int combination channel, both in terms of increased number of identified detections and fewer false alarms. Thus, it is the recommended to use the dual combination channel.

Acronyms

AIS	Automatic Identification System
ASAR	Advanced Synthetic Aperture Radar
CE	Confidence Estimate
CFAR	Constant False Alarm Rate
ENL	Equivalent Number of Looks
ESA	European Space Agency
EW	Extra Wide
FFI	Norwegian Defence Research Establishment
HLOP	High Level Operations Plan
IW	Interferometric Wide
KSAT	Kongsberg Satellite Services
LRIT	Long Range Identification System
LRT	Likelihood Ratio Test
MHT	Multi Hypothesis Tracker
NCA	Norwegian Coastal Administration
NIS	Normalized Intensity Sum
OCWT	Over Complete Wavelet Transform
PCA	Principal Component Analysis
PDF	Probability Density Function
P_{FA}	Probability of False Alarm
SAR	Synthetic Aperture Radar
SLC	Single Look Complex
S1A	Sentinel-1A
S1B	Sentinel-1B

TOPSAR	Terrain Observation with Progressive Scans SAR
VMS	Vessel Monitoring System
WT	Wavelet Transform

References

[1] T. N. Arnesen and R. B. Olsen, "Skipsdeteksjon i SAR data fra sivile radarsatellitter for SATHAV," FFI 00380, 2005.

[2] Ø. Helleren, B. Narheim, Ø. Olsen, R. Olsen, A. N. Skauen, and K. Svenes, "AISSat-1 - System Overview and Performance Analyses," FFI 02083, 2012.

[3] T. N. Hannevik, "Evaluation of RadarSat-2 for ship detection," FFI 01692, 2011.

[4] ESA. (11/12/2017). *http://earth.esa.int/web/sentinel/technical-guides/sentinel-1-sar/products-algorithms/level-1-algorithms/topsar-processing*.

[5] ESA. (11/12/2017). *http://earth.esa.int/web/guest/missions/esa-operational-eo-missions/sentinel-1*.

[6] ESA. (11/12/2017). *http://sentinel.esa.int/web/sentinel/technical-guides/sentinel-1-sar;jsessionid=B6E4DBB0343029BD762D0F2CCB91A7ED.jvm2*.

[7] T. N. Hannevik, K. Eldhuset, and R. B. Olsen, "Improving ship detection by using polarimetric decompositions," FFI 01554, 2015.

[8] R. B. Olsen, K. Eldhuset, Ø. Helleren, and C. Brekke, "MARISS Extension Phase 2," 2009.

[9] C. Liu, "A dual-polarization ship detection algoritm," DRDC DRDC-RDDC-2015-R109, 2015.

[10] C. Liu, P. W. Vachon, and G. W. Geling, "Improved ship detection with airborne polarimetric SAR data," *Canadian Journal of Remote Sensing*, vol. 31, pp. 122-131, 2005.

[11] D. J. Crisp, "A ship detection system for RADARSAT-2 dual-pol multi-look imagery implemented in the ADSS," presented at the International Conference on Radar, Adelaide, Australia, 2013.

[12] A. J. E. Smith, J. Chesworth, and H. Greidanus, "SHIP DETECTION WITH ENVISAT'S ALTERNATING POLARIZATION MODE," in *Envisat & ERS Symposium*, Salzburg, Austria, 2004.

[13] X. Li and J. Chong, "Processing of Envisat Alternating Polarization Data for Vessel Detection," *IEEE Geoscience and Remote Sensing Letters*, vol. 5, pp. 271-275, 2008.

[14] R. Pelich, G. M. R. Garello, N. Longépé, and G. Hajduch, "Ship detection with the Hölder moments and SAR dual-pol data," presented at the International Symposium on Electronics and Telecommunications (ISETC), Timisoara, 2016.

[15] M. Tello, C. López-Martínez, and J. J. Mallorqui, "Automatic vessel monitoring with single and multidimensional SAR images in the wavelet domain," *ISPRS Journal of Photogrammetry and Remote Sensing*, vol. 61, pp. 260-278, 2006.

[16] C. Theoharatos, A. Makedonas, N. Fragoulis, V. Tsagaris, and S. Costicoglou, "DETECTION OF SHIP TARGETS IN POLARIMETRIC SAR DATA USING 2D-PCA DATA FUSION," *Int. Arch. Photogramm. Remote Sens. Spatial Inf. Sci.*, vol. XL-7/W3, pp. 1017-1024, 2015.

[17] S. Song and J. Yang, "Ship detection in polarimetric SAR iamges via tensor robust principle component analysis," presented at the Geoscience and Remote Sensing Symposium (IGARSS), Milano, Italy, 2015.

[18] T. N. Hannevik and R. B. Olsen, "Aegir installation and user manual," FFI 01858, 2013.

[19] C. Brekke, "Automatic ship detection based on satellite SAR," FFI 00847, 2008.

[20] H. Greidanus and C. Santamaria, "First Analyses of Sentinel-1 Images for Maritime Surveillance," JRC JRC92666, 2014.

[21] H. Knutsen, "Product of two K-distributions," FFI 17/16253, 2017.

[22] Wikipedia. (2017). *https://en.wikipedia.org/wiki/Chi-squared_test*.
[23] E. Messel, K. Landmark, and A. Ommundsen, "Implementasjon av en nettbasert prosesseringstjeneste for automatisk skipsidentifisering i bilder fra radarsatellitter," FFI 01554, 2014.
[24] "Oral communication with Richard Olsen, November 2017," ed.
[25] T. N. A. Hannevik and R. B. Olsen, "Automatic ship detection and confidence estimates," FFI 17/01317, 2017.

About FFI

The Norwegian Defence Research Establishment (FFI) was founded 11th of April 1946. It is organised as an administrative agency subordinate to the Ministry of Defence.

FFI's MISSION

FFI is the prime institution responsible for defence related research in Norway. Its principal mission is to carry out research and development to meet the requirements of the Armed Forces. FFI has the role of chief adviser to the political and military leadership. In particular, the institute shall focus on aspects of the development in science and technology that can influence our security policy or defence planning.

FFI's VISION

FFI turns knowledge and ideas into an efficient defence.

FFI's CHARACTERISTICS

Creative, daring, broad-minded and responsible.

Om FFI

Forsvarets forskningsinstitutt ble etablert 11. april 1946. Instituttet er organisert som et forvaltningsorgan med særskilte fullmakter underlagt Forsvarsdepartementet.

FFIs FORMÅL

Forsvarets forskningsinstitutt er Forsvarets sentrale forskningsinstitusjon og har som formål å drive forskning og utvikling for Forsvarets behov. Videre er FFI rådgiver overfor Forsvarets strategiske ledelse. Spesielt skal instituttet følge opp trekk ved vitenskapelig og militærteknisk utvikling som kan påvirke forutsetningene for sikkerhetspolitikken eller forsvarsplanleggingen.

FFIs VISJON

FFI gjør kunnskap og ideer til et effektivt forsvar.

FFIs VERDIER

Skapende, drivende, vidsynt og ansvarlig.

FFI's organisation

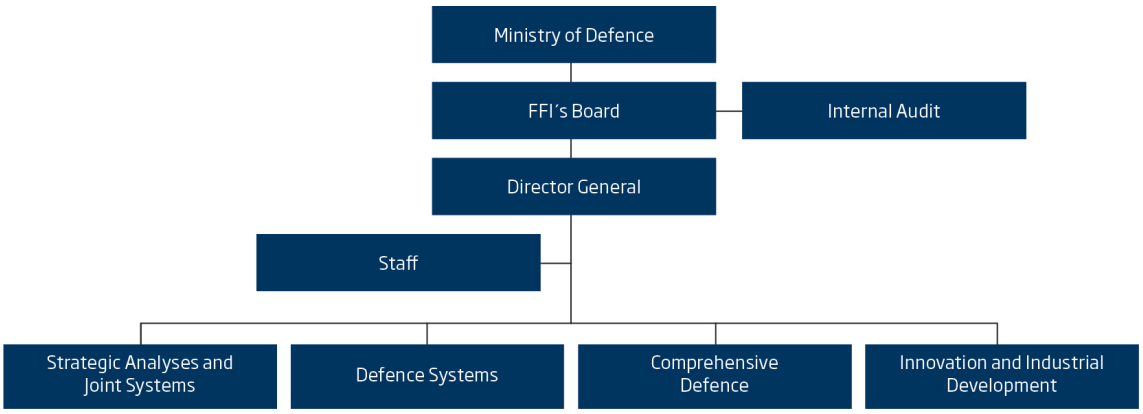

Forsvarets forskningsinstitutt
Postboks 25
2027 Kjeller

Besøksadresse:
Instituttveien 20
2007 Kjeller

Telefon: 63 80 70 00
Telefaks: 63 80 71 15
Epost: ffi@ffi.no

Norwegian Defence Research Establishment (FFI)
P.O. Box 25
NO-2027 Kjeller

Office address:
Instituttveien 20
N-2007 Kjeller

Telephone: +47 63 80 70 00
Telefax: +47 63 80 71 15
Email: ffi@ffi.no

FFI Forsvarets forskningsinstitutt
Norwegian Defence Research Establishment